

Human Action Recognition from Various Data Modalities: A Review

Zehua Sun, Jun Liu, Qihong Ke, and Hossein Rahmani

Abstract—Human Action Recognition (HAR), aiming to understand human behaviors and then assign category labels, has a wide range of applications, and thus has been attracting increasing attention in the field of computer vision. Generally, human actions can be represented using various data modalities, such as RGB, skeleton, depth, infrared sequence, point cloud, event stream, audio, acceleration, radar, and WiFi, etc., which encode different sources of useful yet distinct information and have various advantages and application scenarios. Consequently, lots of existing works have attempted to investigate different types of approaches for HAR using various modalities. In this paper, we give a comprehensive survey for HAR from the perspective of the input data modalities. Specifically, we review both the hand-crafted feature-based and deep learning-based methods for single data modalities, and also review the methods based on multiple modalities, including the fusion-based frameworks and the co-learning-based approaches. The current benchmark datasets for HAR are also introduced. Finally, we discuss some potentially important research directions in this area.

Index Terms—Action Recognition, Hand-crafted Feature, Deep Learning, Data Modality, Single modality, Multi-modality, Dataset.



1 INTRODUCTION

HUMAN Action Recognition (HAR), i.e., understanding and recognizing the human actions, is crucial in plenty of real-world applications. It can be used in visual surveillance systems [1] to identify dangerous human activities, and can also be used in autonomous navigation systems [2] to understand human behaviors for safe operation alongside humans. Besides, HAR is also important for video retrieval [3], human-robot interaction [4], entertainment, and so on.

In the early days, most of the works focused on using RGB (or gray-scale) videos as inputs for HAR [5], due to their popularity in daily life. Recent years have witnessed an emergence of works using other data modalities [6], [7], [8], [9], [10], [11], [12], [13], [14], [15], including skeleton, depth, infrared sequence, point cloud, event stream, audio, acceleration, radar, and WiFi, etc., for HAR. This is mainly thanks to the development of different kinds of accurate and affordable sensors (such as Kinect), and the distinct advantages of different data modalities for HAR in various application scenarios.

Specifically, according to the visibility, data modalities can be roughly divided into visual modalities and sensor modalities. RGB, skeleton, depth, infrared sequence, point cloud, and event stream are visually ‘intuitive’ for representing human actions, and can be seen as visual modalities. Generally, visual modalities are very intuitive and effective for HAR. Among them, RGB video data is the most common data type for HAR, which has been widely

used in surveillance and monitoring systems. Skeleton data encoding trajectories of human body joints, is succinct and efficient for HAR when the action does not involve objects or scene context. Depth and point cloud data record the 3D structure and distance information, which is popularly used for HAR in robot navigation and self-driving applications. Besides, infrared sequence data can be utilized for HAR in even dark environments, while event stream keeps the foreground movement of the humans and avoids much visual redundancy, and thus is also suitable for HAR. Meanwhile, audio, acceleration, radar, and WiFi, etc., are sensor modalities, which though are not so visually ‘intuitive’, yet can be used to recognize actions in some scenarios while protecting the privacy of subjects. Among them, audio data is suitable for locating actions in the temporal sequence, while acceleration data can be utilized for fine-grained HAR. For example, acceleration information can be used to perform quantitative gait analysis [16]. Besides, as a sensor modality, radar data can even be utilized for through-wall HAR. More details of different modalities are discussed in Section 3 of this review paper.

Single modality-based HAR has been extensively investigated in the past decades. Besides, since different modalities have different strengths and limitations for HAR, analyzing the fusion of multiple data modalities and transferring knowledge across modalities have also received great attention recently, so as to enhance the accuracy and robustness of HAR. More specifically, fusion means fusing information of two or more modalities to recognize actions. For example, audio data can serve as the complementary information of visual modalities for HAR (e.g., ‘put plate’ versus ‘put bag’) [17]. Besides, some methods focused on co-learning, i.e., transferring knowledge across different modalities to strengthen the robustness of HAR models. For example, in [18], both RGB and depth data were utilized during training, while recognition can still be reliably per-

- Z. Sun is with Singapore University of Technology and Design, Singapore. E-mail: sunembrace@whu.edu.cn.
- J. Liu is with Singapore University of Technology and Design, Singapore. E-mail: jun_liu@sutd.edu.sg.
- Q. Ke is with The University of Melbourne, Australia. E-mail: qihong.ke@unimelb.edu.au.
- H. Rahmani is with Lancaster University, UK. E-mail: h.rahmani@lancaster.ac.uk.
- Corresponding author: Jun Liu (jun_liu@sutd.edu.sg).

formed when only one modality is available during testing.

Considering the significance of using different single modalities for HAR, and also leveraging their complementary characteristics for fusion and co-learning-based HAR, in this paper, we review existing HAR methods from the perspective of data modalities. In particular, we review the hand-crafted feature-based and deep learning methods that use single modalities, including RGB, skeleton, depth, infrared sequence, point cloud, event stream, audio, acceleration, radar, WiFi, and other modalities, for HAR. We also review the works using multiple modalities for HAR, including the fusion methods and the co-learning approaches. Benchmark datasets for HAR are also reviewed in this paper. The taxonomy of this paper is shown in Figure 1.

Below we summarize the main contributions of this paper:

- To the best of our knowledge, this is the first survey paper that comprehensively reviews the HAR methods from the perspective of various data modalities, including RGB, depth, skeleton, infrared sequence, point cloud, event stream, audio, acceleration, radar, and WiFi, etc.
- To the best of our knowledge, this is the first survey paper that comprehensively covers multi-modality-based HAR methods, and categorizes them into two categories, namely, multi-modality fusion-based methods and cross-modality co-learning-based methods.
- This paper covers both the hand-crafted feature-based and deep learning methods for HAR, especially the most recent and advanced progress of deep learning on HAR.
- Comprehensive comparisons of existing methods on several publicly available datasets are provided (e.g., in Tables 2, 3, and 4), with brief summaries and insightful discussions being presented.

The structure of this paper is as follows. Section 2 reviews the existing survey papers for HAR. Section 3 reviews HAR methods using single data modalities. Section 4 reviews the works using multi-modality data for HAR, including multi-modality fusion and cross-modality co-learning methods. Section 5 lists benchmark datasets. Section 6 discusses the potential future development of HAR. Specifically, we compare different data modalities. Then we review HAR works using RGB, depth, skeleton, infrared sequences, point cloud, audio, acceleration, radar, WiFi, and other modalities that are not classified in the above categories.

2 RELATED WORKS

In this section, we briefly review the existing survey papers on HAR. There have been plenty of general survey papers for HAR [19], [20], [21], [22], [23], [24], [25], [26], [27]. Lun and Zhao [19] gave a survey of HAR using Microsoft Kinect [28] with the template-based and algorithmic-based methods. Wang et al. [27] analyzed and compared ten Kinect-based HAR algorithms. Zhang et al. [20] summarized the benchmark RGB-Depth datasets, including single-view,

multi-view, and multi-person datasets. The works of [21], [22] reviewed hand-crafted feature-based and deep learning methods for HAR in video sequences. Koozhadi and Charkari [23] discussed the deep learning methods for HAR in a comparative form. Kong et al. [24] gave a survey about action recognition and prediction tasks. Wang et al. [25] gave an overview of HAR methods using Convolutional Neural Networks (CNNs) and Recurrent Neural Networks (RNNs) based on RGB-D data, and they grouped the methods into the segmented sequence and continuous sequence-based ones. Zhang et al. [26] presented a comprehensive survey of human action analysis, including recognition, interaction, and detection. Jegham et al. [29] studied the challenges and corresponding characterization methods to address the issues in HAR. Apart from the aforementioned surveys, some other papers focused on reviewing existing methods based on one specific data modality, as follows.

Surveys focusing on RGB-based HAR. Some survey papers focused on discussing methods using the RGB modality for HAR [5], [30], [31], [32], [33], [34]. Poppe [5] reviewed the hand-crafted feature-based methods for video-based HAR. Weiland et al. [31] mainly reviewed the methods of action representation, segmentation, and recognition. In the work of [32], the activity recognition methods were divided into two categories: single-layered and hierarchical approaches. The former is the recognition of gestures and actions with sequential characteristics, while the latter represents high-level activities. Video datasets were reviewed in [33]. Guo and Lai [34] gave a survey about the recognition from still images.

Surveys focusing on skeleton-based HAR. Some survey papers reviewed methods that use the skeleton modality for HAR [35], [36], [37], [38]. Presti and Cascia [36] reviewed technologies and approaches for 3D skeleton-based action classification. Han et al. [37] focused on space-time representations of actions, and gave a categorization from four perspectives, namely, information modality, representation encoding, structure and topological transition, and feature engineering. Recently, Ren et al. [38] gave a comprehensive survey on 3D skeleton-based HAR using deep learning networks, especially CNNs, RNNs, and Graph Convolutional Networks (GCNs).

Surveys focusing on depth-based HAR. Some surveys reviewed methods on depth-based HAR [35], [39], [40], [41]. Chen et al. [39] gave a review of using depth imagery for analyzing human activities. Approaches of depth-based and skeleton-based HAR were reviewed in [40]. Aggarwal and Xia [35] summarized the HAR methods using 3D data with a focus on techniques using depth data.

Surveys focusing on sensor-based HAR. Some survey papers reviewed methods on sensor-based HAR [41], [42], [43], [44], [45], [46], [47], [48], [49]. Avci et al. [42] introduced five major steps for the HAR process using inertial sensors, which include pre-processing, segmentation, feature extraction, dimensionality reduction, and classification. Chen et al. [43] reviewed the approaches for sensor-based action monitoring, modeling, and recognition, respectively. In the work of [45], approaches based on mobile phones were reviewed. The thrust of [41] was on depth cameras and inertial sensors. Wang et al. [47] surveyed sensor-based deep learning HAR methods. Besides, some other surveys

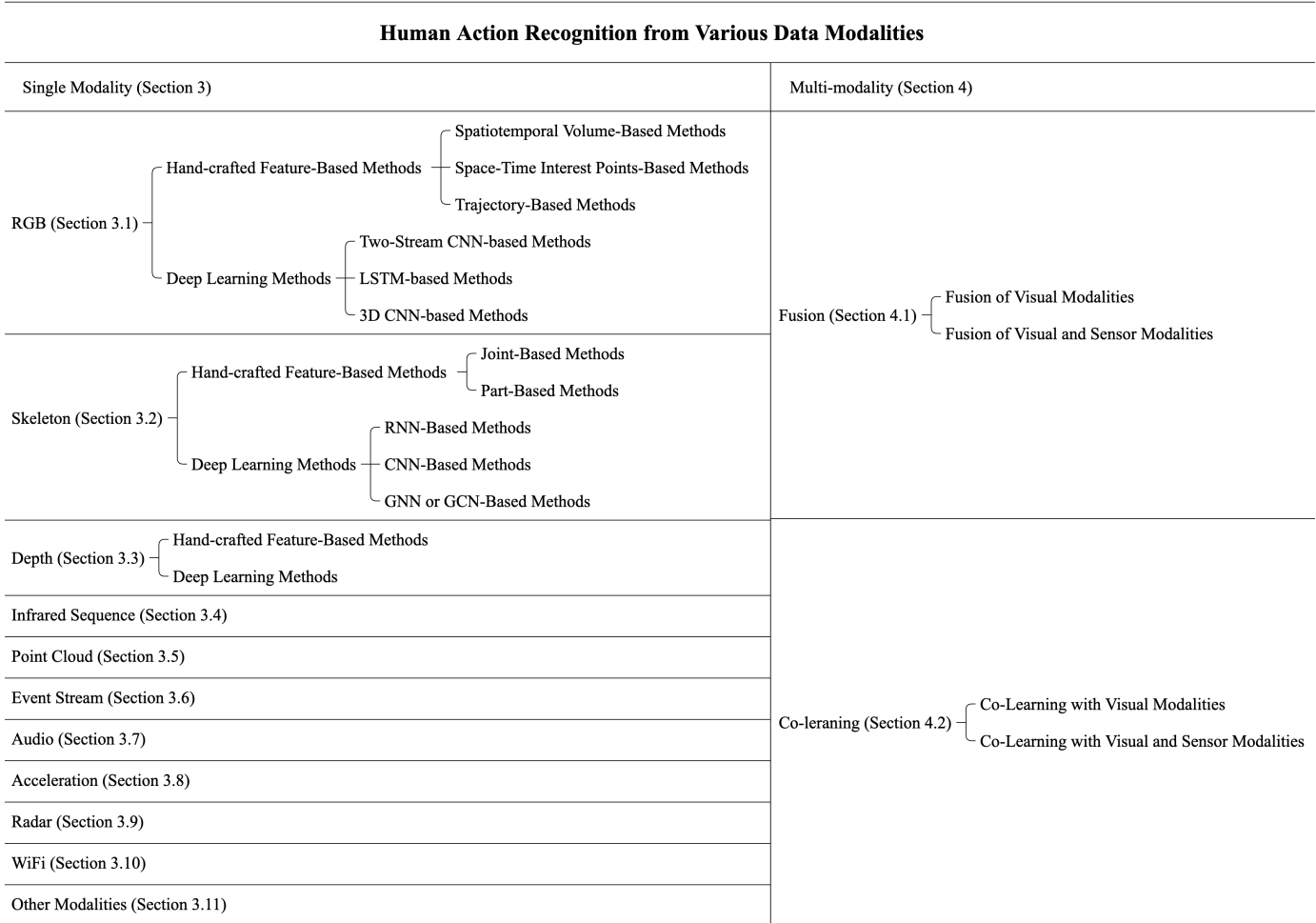


Fig. 1. A taxonomy of human action recognition from various data modalities.

focused on acceleration [48], WiFi [46], and radar data [49] as well.

Compared to the above survey papers, we comprehensively review methods on HAR from the perspective of various input data modalities, including RGB, depth, skeleton, infrared sequence, point cloud, event stream, audio, acceleration, radar, and WiFi, etc., which makes our survey unique. Specifically, we not only provide a comprehensive review of HAR methods using single data modalities, but also discuss HAR methods based on multiple modalities, including the multi-modality fusion methods and the cross-modality co-learning methods.

3 SINGLE MODALITY

Existing methods [6], [7], [8], [9], [10], [11], [12], [13], [14], [15] have exploited various data modalities for HAR. In this section, we review HAR methods based on RGB, skeleton, depth, infrared sequence, point cloud, event stream, audio, acceleration, radar, WiFi, and other modalities. TABLE 1 gives action samples of different data modalities and summarizes their corresponding advantages and disadvantages.

Specifically, we summarize both the hand-crafted feature-based methods and deep learning methods using single data modalities for HAR in this section. The hand-crafted feature-based methods generally consist of two

steps, namely, feature extraction and action classification with the features, while deep learning methods often integrate feature learning and classification into one network, which are quite effective for HAR and have become the mainstream in this field.

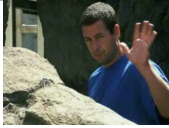

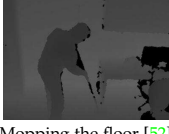


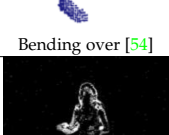

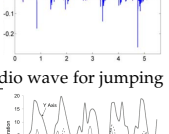
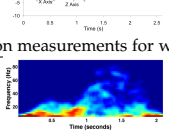
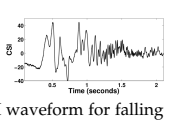
3.1 RGB MODALITY

Human eyes are sensitive to three main wavelengths of light, i.e., red, green, and blue (RGB) [59]. The combinations of different amounts of the three basic colors result in various colors. The RGB modality generally refers to the images or videos (sequences of images) captured by RGB cameras, which aim to recreate what human eyes see.

The RGB modality is easy to collect and contains rich appearance information of the scene context. HAR using the RGB modality has a wide range of applications such as visual surveillance [60], autonomous navigation [61], sports analysis [62], etc. However, HAR from the RGB modality is challenging, due to the large variations of backgrounds, viewpoints, scales of humans, and illumination conditions existing in the RGB data. Besides, RGB videos generally have a large data size, leading to high computational cost when modeling the spatio-temporal context information.

In this subsection, we review methods using the RGB modality for HAR. Specifically, since videos contain tempo-

TABLE 1
Samples of different data modalities with corresponding pros and cons.

Modality	Example	Pros	Cons
Visual Modality	RGB  Hand-waving [50]	<ul style="list-style-type: none"> · Rich appearance information · Easy to obtain and operate · Wide applications 	<ul style="list-style-type: none"> · Sensitive to view · Sensitive to background · Sensitive to illumination · Complex computations
	3D Skeleton  Looking at the watch [51]	<ul style="list-style-type: none"> · 3D structure information of the subject · Simple yet informative · Insensitive to view · Insensitive to background 	<ul style="list-style-type: none"> · Lack of color and texture information · Lack of detailed shape information · Noisy
	Depth  Mopping the floor [52]	<ul style="list-style-type: none"> · 3D structure information · Geometric shape information · Workable in dark environments 	<ul style="list-style-type: none"> · Lack of color and texture information
	Infrared Sequence  Pushing [53]	<ul style="list-style-type: none"> · Workable in dark environments 	<ul style="list-style-type: none"> · Lack of color and texture information · Susceptible to sunlight
	Point Cloud  Bending over [54]	<ul style="list-style-type: none"> · 3D information · Geometric information · Insensitive to view 	<ul style="list-style-type: none"> · Lack of color and texture information · Sparse representation
	Event Stream  Running [55]	<ul style="list-style-type: none"> · Avoiding visual redundancy · High dynamic range · No motion blur 	<ul style="list-style-type: none"> · Asynchronous output · Spatio-temporally sparse · Relatively expensive device
Sensor Modality	Audio  Audio wave for jumping [56]	<ul style="list-style-type: none"> · Easily locating actions in temporal sequence 	<ul style="list-style-type: none"> · Lack of rich information
	Acceleration  Acceleration measurements for walking [57]	<ul style="list-style-type: none"> · Recognize fine-grained actions · Privacy protecting 	<ul style="list-style-type: none"> · Need to carry devices
	Radar  Spectrogram for falling [58]	<ul style="list-style-type: none"> · Can be used for through-wall HAR · Privacy protecting 	<ul style="list-style-type: none"> · Relatively expensive device
	WiFi  CSI waveform for falling [58]	<ul style="list-style-type: none"> · No need to carry devices · Simplicity and convenience · Privacy protecting · Low cost 	<ul style="list-style-type: none"> · Noisy · Small range of the space

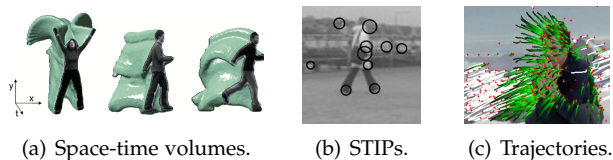


Fig. 2. An illustration of three types of RGB-based hand-crafted features for HAR, including (a) space-time volumes, (b) space-time interest points (STIPs), and (c) trajectories. (a)-(c) are originally shown in [66], [67], [68].

ral dynamics of human motions that are crucial for HAR, most of the existing methods used videos for HAR [33], while only a few works focused on using static images [63], [64], [65]. Consequently, here we focus on RGB video-based HAR methods, and review both the hand-crafted feature-based and deep learning works using RGB videos.

3.1.1 Hand-crafted Feature-Based Methods

Generally, the first step of hand-crafted feature-based methods is to perform feature extraction. Then the extracted features are used for action classification. As shown in Figure 2, the hand-crafted feature-based methods can be mainly divided into three categories according to the types of the extracted features, i.e., space-time volume-based methods, space-time interest point-based methods, and trajectory-based methods. The space-time volumes belong to holistic representations, i.e., global representations of human body shapes, structures, and motions. The other two types of features are local representations that describe the local regions. Below we review methods based on these three types of features.

Space-Time Volume-Based Methods. As shown in Figure 2(a), the space-time 3D volume is generated from an action video sequence, which contains the information of the spatial human body and temporal dynamics. The general idea of space-time volume-based methods is to construct a 3D space-time template and then use the template to perform matching.

Bobick and Davis [69] proposed a Motion Energy Image (MEI) and a Motion History Image (MHI) as action representations based on silhouettes and images with human regions obtained by background subtraction. Then they developed a method that matches temporal templates for HAR. The MEI and MHI represent where and how motion is moving, respectively. The limitation is that the MEI and MHI are sensitive to view variations. Weinland et al. [70] proposed a Motion History Volumes (MHV), which is a viewpoint-free representation and is more robust to viewpoint variations. The MHV is a great advancement of the holistic representation. Gorelick and Blank et al. [66] utilized properties of the solution to the Poisson equation to extract space-time features. Yilmaz et al. [71] introduced a space-time volume that is a sequence of 2D contour. Each 2D contour is generated by projecting the outer boundary of an object in the image plane. Ali [72] and Efros et al. [73] utilized optical flow rather than the silhouettes to extract motion information for HAR.

The aforementioned space-time volumes are holistic representations, and the holistic methods, i.e., methods based

on the space-time volumes, were popular for a long time. These methods are characterized by intuitive and straightforward representations, but often lack local details. Besides, they are often not robust to various lighting and complex scenes. In addition, the representations used by them are generally high-dimensional, leading to high computational costs. Consequently, researchers have made efforts in designing local representations to handle the issues in the holistic representations.

Space-Time Interest Point (STIP)-Based Methods. The STIPs are local representations, where the main idea is to treat a video as a 3D function, and then map the video into a 1D space through a mapping function. The points with local maximum values in the 1D space are the points of interest. The interesting points (See Figure 2(b)) generally refer to the positions that have the most dramatic changes in spatial and temporal dimensions [74].

Generally, there are four steps in STIP-based HAR approaches, namely, STIPs detection, feature extraction, vocabulary building, and classification [74]. In these methods, the detectors include dense [75] and sparse [67], [76] feature-based detectors. Descriptors such as 3D SIFT [77], HOG3D [78], local trinary patterns [79] were used for feature extraction. For vocabulary building, one of the popular methods is the Bag-of-words (BoW) [80], [81] based framework. Common classifiers are Support Vector Machine (SVM), probabilistic Latent Semantic Analysis (pLSA), Latent Dirichlet Allocation (LDA), Nearest Neighbour Classifier (NNC), etc.

One of the earliest work of STIP-based methods was motivated by the Harris corner detector [82], which extended spatial interest points into the 3D spatio-temporal dimensions [67]. One disadvantage of this method is the lack of stable interest points as spatio-temporal corners are rare. To address this issue, Dollar et al. [76] applied the Gabor filter in the spatial and temporal dimensions. Wong and Cipolla [83] first narrowed the scope of an image to a small set of subspace images, and then detected interest points from the scope, rather than detecting in the entire image. In [84], a few sparse methods and dense sampling methods were compared, where dense sampling was found to be able to outperform many other detectors. As some irrelevant features often affect the result, Liu et al. [85] utilized motion cues to prune the irrelevant features.

The main advantage of the aforementioned STIP-based methods is that the pre-processing step such as segmentation of the background is often not required. These local features are scale and rotation invariant, yet are sensitive to the variations of camera positions and views. Besides, the STIP-based methods are not capable of effectively capturing long-term temporal information, so later on, how to track these interest points became one of the important research directions in hand-crafted feature-based HAR.

Trajectory-Based Methods. The trajectory (See Figure 2(c)) is a kind of features tracked over a period of time. Trajectory-based methods generally utilize the tracking path of key points or the human skeletons to represent actions in long-term duration.

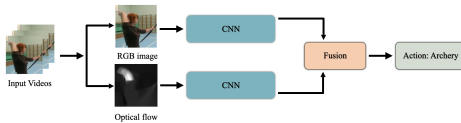
Wang et al. proposed Dense Trajectories (DT) [86] and improved Dense Trajectories (iDT) [68] for HAR, which are classic and representative trajectory-based algorithms. The main steps of the DT algorithm [86] are to use the optical

flow to obtain the trajectory in the video sequence, and then extract Histograms of Optic Flow (HOF) [87], Histograms of Oriented Gradient (HOG) [88], and Motion Boundary Histograms (MBH) [89] features, which are encoded using the Bag of Features (BoF) method [87]. Finally, the encoded features are used to train the SVM classifier for action classification. The iDT algorithm [68] is an improved version of the DT algorithm. Compared to the DT algorithm, the iDT uses L1 normalization to perform feature regularization, and then uses Fisher Vector (FV) to perform feature encoding. In addition, the iDT uses Speeded Up Robust Features (SURF) [90] key-points and dense optical flow to match feature points between frames to eliminate or mitigate the effects of the camera location variations.

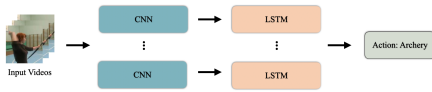
Researchers have also made efforts in further improving the accuracy and effectiveness of the iDT algorithm [91], [92], [93]. Based on iDT, Peng et al. [92] proposed Stacked Fisher Vectors (SFV), i.e., a representation with multi-layer nested Fisher vector encoding, for HAR. They first performed Fisher vector encoding in dense sub-volumes based on low-level features, and then compressed FVs to low dimension and performed another FV encoding. Wang et al. [93] removed the background trajectories, and warped optical flow with an estimated homography approximating the camera motion to improve the accuracy.

3.1.2 Deep Learning Methods

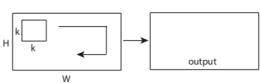
The hand-crafted feature-based methods have shown some promising results for HAR, but they are often not reliable for handling large and challenging datasets. Recent years have seen an increasing number of deep learning methods for HAR. The representative works can be mainly divided into three categories, i.e., two-stream CNN-based, Long Short-Term Memory (LSTM)-based, and 3D CNN-based methods. TABLE 2 compares the performance of the RGB-based deep learning methods on the UCF101 [94], HMDB51 [50], and Kinectis-400 [95] benchmark datasets.



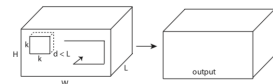
(a) Schema of two-stream CNN-based methods.



(b) Schema of LSTM-based methods.



(c) Schema of 2D convolution.



(d) Schema of 3D convolution.

Fig. 3. An illustration of RGB-based deep learning methods. (a) and (b) illustrate the frameworks of two-stream CNN-based and LSTM-based methods. (c) and (d) illustrate the 2D and 3D convolution operations. (c) and (d) are originally shown in [96].

Two-Stream CNN-Based Methods. As the name suggests, the two-stream CNN network contains two CNN branches, taking different input features extracted from the RGB video for HAR, and the final result is obtained through a fusion strategy, as shown in Figure 3(a).

Karpathy et al. [97] studied how to extend the connectivity of CNN in the time domain to make full use of local spatio-temporal information and proposed a multi-resolution CNN architecture. The input frames are fed into two separate streams, namely, a context stream modeling low-resolution images and a fovea stream processing high-resolution center crops. Simonyan and Zisserman [98] proposed a two-stream CNN architecture that consists of a spatial network and a temporal network. Specifically, given the RGB video, the individual frame of the video and multi-frame optical flow calculated from the video are respectively inputted into the spatial stream CNN and the temporal stream CNN. The outputs of the two streams are then fused to generate the final recognition result.

Plenty of studies endeavored to make an extension and improvement for two-stream CNN. Wang et al. [101] proposed a Trajectory-pooled Deep-convolutional Descriptor (TDD) to represent videos, incorporating the merits of both hand-crafted features and deep-learned features. In particular, they extracted multi-scale convolutional feature maps using the two-stream network, and TDD descriptors were then calculated by trajectory-constrained sampling and pooling. To model the long-range temporal structure, Wang et al. [106] proposed a novel framework for HAR, termed as Temporal Segment Network (TSN). TSN involves the idea of sparse temporal sampling and video-level supervision, where one short snippet is randomly selected from several divided segments of the input video, and the class scores of different snippets are fused to obtain the video-level prediction. [114], [151] made some improvements to TSN as well. Cheron et al. [99] proposed a Pose-based CNN (P-CNN) descriptor that aggregates motion and appearance information along the tracks of the human body. Wang et al. [103] designed a Siamese network to model actions as a transformation that changes the environmental state (precondition) before the action to the state (effect) after the action, where precondition and effect are the inputs to the two-stream network. For example, the precondition of kicking a ball is that the player runs towards the ball, and the effect is that the ball flies away. Wang et al. [104] introduced semantics cues (e.g., scenes, persons, and objects), and proposed a two-stream Semantic Region-based CNNs (SR-CNNs). In [113], the appearance and motion pathways were fed into a two-stream architecture coupled with injected identity mapping kernels for learning long-term relationships. Diba et al. [115] embedded Temporal Linear Encoding (TLE) as a new layer inside of CNNs to capture the appearance and motion throughout entire videos, and the scores for the two CNNs were combined by averaging, i.e., this method encodes the aggregated information into a global feature representation for end-to-end learning. Zhu et al. [116] introduced a novel CNN architecture named hidden two-stream networks to implicitly capture the motion information between adjacent frames to capture the temporal relationships. Feichtenhofer et al. [117] designed a special two-stream network termed as SlowFast network, where one stream is a Slow pathway

TABLE 2

Performance comparison of RGB-based deep learning methods for HAR on the UCF101, HMDB51, and Kinetics-400 benchmark datasets. For simplicity, the '%' after the value is omitted. The symbol '-' indicates that the result is unavailable.

	Method	Reference	Year	Dataset		
				UCF101	HMDB51	Kinetics-400
Two-stream CNN-Based	Multiresolution CNN	[97]	2014	65.4	-	-
	Two-stream CNN+SVM	[98]	2014	88.0	59.4	-
	P-CNN	[99]	2015	-	-	-
	Very deep two-stream	[100]	2015	91.4	-	-
	TDD+iDT	[101]	2015	91.5	65.9	-
	EMV+RGB-CNN	[102]	2016	86.4	-	-
	Siamese Network	[103]	2016	92.4	63.4	-
	SR-CNNs	[104]	2016	92.6	-	-
	Feichtenhofer et al.	[105]	2016	93.5	69.2	-
	TSN	[106]	2016	94.2	69.4	-
	ST-ResNet*+iDT	[107]	2016	94.6	70.3	-
	Girdhar et al.	[108]	2017	-	52.2	-
	STPP	[109]	2017	92.6	70.5	-
	AdaScan+iDT+C3D	[110]	2017	93.2	66.9	-
	ActionVLAD+iDT	[111]	2017	93.6	69.8	-
	ST-VLMPF	[112]	2017	94.3	73.1	-
	Feichtenhofer et al.	[113]	2017	94.9	72.2	-
	DOVF+MIFS	[114]	2017	95.3	75.0	-
	TLE: Bilinear	[115]	2017	95.6	71.1	-
	Hidden Two-stream CNN+I3D	[116]	2018	97.1	78.7	-
SlowFast	[117]	2019	-	-	79.8	
TSN+SoSR+ToSR	[118]	2019	92.1	68.3	-	
D ³ -LND	[119]	2019	92.8	67.8	-	
Chen et al.	[120]	2019	94.4	67.2	-	
LSF CNN	[121]	2020	94.8	70.2	-	
LSTM-Based	3D CNN+LSTM	[122]	2012	-	-	-
	Soft Attention Model	[123]	2015	-	41.3	-
	LRCNs	[6]	2015	82.9	-	-
	Composite LSTM Model	[124]	2015	84.3 (RGB+flow)	44.0 (RGB)	-
	Yue et al.	[125]	2015	88.6	-	-
	Wu et al.	[126]	2015	91.3	-	-
	sLSTM	[127]	2016	84.0	55.1	-
	DB-LSTM	[128]	2017	91.2	87.6	-
	L ² STM	[129]	2017	93.6	66.2	-
	Ge et al.	[130]	2019	92.8	67.1	-
	Multi-task C3D+LSTM	[131]	2019	93.4	68.9	-
	CNN+TR-LSTM	[132]	2019	-	63.8	-
	STS-ALSTM	[133]	2020	92.7	64.4	-
	C ² LSTM	[134]	2020	92.8	61.3	-
	ResCNN-DBLSTM	[135]	2020	94.8	-	-
3D CNN-Based	Ji et al.	[136]	2012	-	-	-
	F _{st} CN	[137]	2015	88.1	59.1	-
	C3D+iDT+SVM	[96]	2015	90.4	-	-
	LTC+iDT	[138]	2017	92.7	67.2	-
	T3D+TSN	[139]	2017	93.2	63.5	62.6 (T3D)
	Two-Stream I3D	[140]	2017	93.4	66.4	78.7
	Two-Stream I3D, Kinetics pre-training	[140]	2017	97.9	80.2	-
	P3D ResNet+iDT	[141]	2017	93.7	-	-
	ARTNet with TSN	[142]	2018	94.3	70.9	78.7
	Two-stream MiCT-Net	[143]	2018	94.7	70.5	-
	ECO_En	[144]	2018	94.8	72.4	76.3
	STC-ResNext 101 (64 frames)	[145]	2018	96.5	74.9	68.7 (32 frames)
	R(2+1)D-TwoStream	[146]	2018	97.3	78.7	75.4
	Asymmetric 3D-CNN	[147]	2019	92.6	65.4	-
	3D CNN Ensemble+iDT	[148]	2020	92.7	69.1	-
	STDA-ResNeXt-101	[149]	2020	95.5	72.7	-
	D3D Ensemble	[150]	2020	97.6	80.5	76.5 (D3D+S3D-G)

operating at the low frame rate, the other is a Fast pathway operating at the high frame rate. The Slow pathway is to capture spatial semantics, while the Fast pathway is to capture the fast-changing motion but with fewer spatial details. Besides, plenty of studies introduced attention mechanisms based on two-stream networks to obtain better recognition results [108]. Recently, some researches also utilized hybrid network architectures involving two-stream architectures and other networks such as LSTM [121], [152], [153] and GCN [154] for HAR. Other two-stream CNN-based methods include [119], [120].

One important problem in the two-stream architectures is how to combine the information of the two streams to

obtain optimal recognition results. Researchers have studied different fusion methods to address this problem [97], [105], [106], [111], [112]. Feichtenhofer et al. [105] studied several ways of fusion, and found it effective to fuse at the last convolution layer of the network for saving parameters without loss of accuracy. Girdhar et al. [111] proposed an end-to-end trainable two-stream network involving the ActionVLAD (a spatio-temporal extension of the NetVLAD [155] aggregation layer) pooling layer, through which the features are pooled across space and time. They experimented with ActionVLAD using concatenation, early, and late fusion strategies, where the late fusion performs the best. Residual connections have also been investigated,

showing good performance [107].

There are also some works addressing other problems in the two-stream CNN architectures. Zhang et al. [102] utilized the motion vector to replace the computationally expensive optical flow information. Then they transferred the knowledge trained with optical flow CNN to motion vector CNN to make up for the low accuracy. Wang et al. [100] found that many two-stream CNNs were relatively shallow, and then they presented very deep two-stream CNNs to address this problem. They pointed out that the deeper network and larger amount of data generally yielded better results of recognition. Considering that many frames of the video sequences are irrelevant or useless for HAR, Kar et al. [110] proposed an adaptive temporal pooling method, i.e., AdaScan, which learns to pool discriminative and informative frames using a single temporal scan of the video. This method helps remove useless frames. Most CNN architectures require inputs to be fixed-sized and fixed-length. Considering that this is not flexible for HAR, Wang [109] introduced an end-to-end framework that is capable of taking videos of arbitrary sizes and lengths as inputs. To address the problem of HAR using videos at low spatial resolutions, Zhang et al. [118] studied the super-resolution problem of video for HAR.

Two-stream CNNs learn spatial and temporal information of the input in two separate networks, and then fuse them to get the final results. Such a method makes up for the shortcomings of traditional 2D CNNs in handling video data, and thus achieves high recognition accuracy. However, this type of architecture is not very powerful for long-term dependency modeling, i.e., it has limitations in modeling temporal context information, while LSTM can make up for it.

LSTM-Based Methods. LSTM-based methods utilize LSTMs to process sequences of ordered video frames for long-term HAR. As shown in Figure 3(b), LSTM-based methods usually use the LSTM with other networks to combine advantages of different networks.

Baccouche et al. [122] trained a 3D CNN followed by an LSTM model with a classifier for HAR. Ng et al. [125] extracted frame-level features from a pre-trained CNN, and then input these features along with optical flow features into a pooling framework or LSTM for training to obtain the final classification results. Donahue et al. [6] proposed Long-term Recurrent Convolutional Networks (LRCNs), consisting of CNNs and LSTMs to process variable-length visual inputs in spatial and temporal dimensions, where the CNNs extract visual features from each time-step of the input, and the LSTMs process the sequence of features to generate the output sequence. In [124], an encoder LSTM was utilized to map an input sequence into a fixed-length representation which was decoded through decoder LSTMs to perform the tasks of reconstructing the input sequences or predicting the future sequences. Wu et al. [126] proposed a hybrid framework that contains a CNN to extract spatial and short-term motion features, and an LSTM to learn longer-term temporal cues. Besides, Majd and Safabakhsh [134] proposed C²LSTM that incorporates the two basic operators of convolution and cross-correlation, to cover the motion and spatial features while extracting the temporal dependencies. There are also some other works focusing on further improving the LSTM-

based HAR network design [129], [131], [156], [157]. As a variant of LSTM, the Bidirectional LSTM, is also popular in HAR [128], [135].

The introduction of the attention mechanisms also helps to better capture the long-term temporal dependency of videos [123], [127], [130], [133]. Sharma et al. [123] added recurrent soft attention to multi-layered RNNs with LSTM units, showing good results. Considering that RNN and LSTM models are computationally expensive when dealing with high dimensional input data, Pan et al. [132] proposed a TR-LSTM, utilizing the low-rank tensor ring decomposition to reformulate the input-to-hidden transformation to reduce computational cost.

Generally, LSTM-based methods are hybrid networks based on LSTM and other existing models. The capability of LSTM in modeling long short-term temporal context information also makes it widely used for HAR with other data modalities, such as the skeleton modality introduced in Section 3.2.

3D CNN-Based Methods. Plenty of researchers extended 2D CNNs into 3D spatio-temporal structures for HAR. Compared to 2D CNNs, there is an additional dimension in 3D CNN to model temporal information, such that 3D convolution enables the network to simultaneously learn both spatial and temporal features for HAR. Figure 3(c) and 3(d) illustrate the 2D and 3D convolution operations, respectively.

Ji et al. [136] developed a novel 3D CNN model to perform 3D convolution from contiguous frames to extract features in both spatial and temporal dimensions, which obtained superior performance for HAR. Tran et al. [96] proposed C3D, consisting of 8 convolutional, 5 max-pooling, 2 fully connected, and 1 softmax layers, and all the 3D convolutional kernels are $3 \times 3 \times 3$ with stride 1 in spatial and temporal dimensions. The features extracted by the C3D are generic, compact, efficient, and simple. However, the C3D network is relatively shallow and is not very suitable for processing long-term data sequence. To this end, [140], [141] proposed deeper networks to further improve the capability of 3D CNNs. Carreira and Zisserman [140] introduced a new two-stream Inflated 3D ConvNet (I3D) by adding the time dimension based on 2D CNN inflation. In their work, they compared I3D with four extra different architectures, namely, LSTM with CNNs, 3D CNNs, two-stream networks, and 3D-fused two-stream networks. Compared to the former 3D CNNs, I3D has fewer parameters and can use the pre-trained networks. Qiu et al. [141] utilized $1 \times 3 \times 3$ convolutional filters on spatial domain plus $3 \times 1 \times 1$ convolution constructing temporal connections between contiguous frames to simulate $3 \times 3 \times 3$ convolutions, and they proposed a Pseudo 3D Residual Network (P3D ResNet) for HAR. Varol et al. [138] proposed a Long-term Time Convolution (LTC) framework that increases the time range of the representation at the cost of reducing the spatial resolution to model long-term sequences. Diba et al. [145] introduced a new block, Spatio-Temporal Channel Correlation (STC), embedded in some architectures such as ResNext and ResNet, which can model the correlations between channels of a 3D CNN with respect to temporal and spatial features. Besides, Li et al. [149] introduced a spatio-temporal deformable CNN module with the attention mechanism to capture long-

range and long-distance dependencies of videos. Inspired by transfer learning, Stroud et al. [150] proposed a Distilled 3D Network (D3D), consisting of a student network and a teacher network, where the student network is trained from RGB videos and also distilling knowledge from the teacher network trained from optical flow sequences. Besides, 2D and 3D CNNs are fused for HAR in [158].

Training 3D CNNs requires a high complexity of calculations and a large amount of data when the network is very deep. Plenty of works focused on reducing the computational cost of training 3D CNNs. Some studies found that factorizing 3D convolution could not only decrease the computational cost [137], but also significantly gain accuracy [146]. Sun et al. [137] proposed a factorized spatio-temporal CNN ($F_{st}CN$), factorizing the 3D convolution learning to learn 2D spatial convolutional layers followed by 1D temporal convolutional layers. Diba et al. [139] extended the DenseNet [159] architecture with 3D filters and pooling kernels, named Temporal 3D ConvNet (T3D), where the temporal transition layer can model variable temporal convolution kernel depths. Specifically, T3D can densely and efficiently capture the appearance and temporal information at short, middle, and long-range terms. As T3D contains more trainable parameters than DenseNet, transfer learning is also considered to decrease the computational cost. Multi-scale temporal convolutions are also utilized to reduce the complexity of 3D convolutions [160]. Yang et al. [147] proposed an asymmetric 3D CNN, and utilized multi-sources enhanced input to decrease the computational cost. Recent researches such as [143], [144], [148], [161] worked for decreasing the computational cost as well.

The 3D CNN-based methods are very powerful in learning discriminative features from both spatial and temporal dimensions for HAR. Though superior performance has been achieved, 3D CNN-based frameworks often contain a large number of parameters, and the network scales are often large.

Apart from the above-mentioned network architectures, some other frameworks have also been designed and applied for HAR in RGB videos, such as temporal convolution-based networks [162], transformer networks [163], and Convolutional Gated Restricted Boltzmann Machines [164], etc.

In general, RGB data is the most commonly used modality for HAR in real-world application scenarios, as it is easy to collect and contains rich information, yet it often requires complex computation for feature extraction. Besides, due to the sensitiveness of the RGB modality w.r.t viewpoint variations and backgrounds, etc., recently, HAR with other modalities, such as 3D skeleton data, have also received great attention, which are introduced in the subsequent sections.

3.2 SKELETON MODALITY

The skeleton sequence encoding the trajectories of human body joints represents the human motions, and thus can be used for HAR. Skeleton data can be acquired using pose estimation and tracking algorithms with RGB [165], [166], [167], [168] and depth data [169], [170], [171], [172], [173], [174]. It can also be collected from motion capture systems. Generally, human pose estimation is sensitive to viewpoint

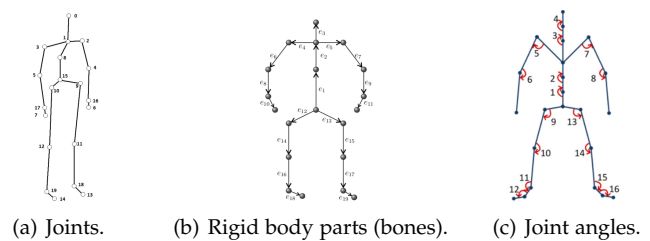


Fig. 4. An illustration of skeleton-based hand-crafted feature representations in (a) joint-based, and (b)(c) part-based methods. The joint-based methods extract features based on the positions and relations of different joints, while the part-based methods extract features based on the information and relations of rigid body parts (bones). (a)-(c) are originally shown in [181], [182], [183].

variations. Meanwhile, motion capture systems, that are insensitive to view and lighting, can provide reliable pose (skeleton) data. However, it is often not convenient to deploy motion capture systems in many practical application scenarios. Thus many recent skeleton-based HAR works [175], [176], [177] used the skeleton data acquired with pose estimation and tracking algorithms using depth maps (e.g., NTU RGB+D dataset [178]) or RGB videos (e.g., Kinetics-skeleton dataset [175]).

There are many advantages of using the skeleton modality for HAR, thanks to the provided body structure and pose information, the essentially simple and informative representation, the scale invariance, the robustness against the variance of clothing texture and background, etc. Due to these advantages and the availability of the accurate and low-cost depth sensors (such as Kinect), skeleton-based HAR has attracted lots of attention in the community recently.

3.2.1 Hand-crafted Feature-Based Methods

In skeleton-based HAR, some of the existing methods [179], [180] focused on extracting hand-crafted spatial and temporal features from the skeleton sequence for classification. The spatial information mainly refers to the structure of the skeleton in each frame, while the temporal information refers to the dependency information of the skeleton data over different frames. The spatial and temporal features can be extracted based on the joint locations and relations, and also body part (bone) angles and relations. Thus, existing hand-crafted feature-based HAR works using skeleton data can be roughly divided into joint-based and body part-based methods, according to the way of feature extraction.

Joint-Based Methods. Joint-based representations have been very widely used in skeleton-based HAR. The joint-based representations (see Figure 4(a)) model actions based on the relative relationships among the coordinates of joints. Wang et al. [184], [185] proposed an actionlet ensemble model for HAR, where in each frame, pairwise relative positions of the joints are calculated as the 3D joint features, and then Fourier Temporal Pyramid is used to model the temporal evolution, which is robust to noise. Xia et al. [186] extended the approach in [169] to extract 3D skeletal joint locations, and proposed Histograms Of 3D Joint locations (HOJ3D) as a representation of human postures, which are then clustered into several posture visual words, and finally,

the temporal information of the visual words is modeled by discrete Hidden Markov Models (HMMs). Yang et al. [187] introduced EigenJoints based on differences of the joint positions including posture, motion, and offset features. Yang et al. [188] further proposed Accumulated Motion Energy (AME) to select the informative frames, which addresses the problem of noise and high computational cost. Hussein et al. [189] introduced Cov3DJ, a temporal hierarchy of co-variance descriptors to encode the relationship between joint movements and time. Gowayed et al. [190] utilized Histogram of Oriented Displacements (HOD) projected by three views to describe 3D joint trajectories, which is scale-invariant and speed-invariant. Other joint-based methods include [179], [180], [181], [191].

Part-Based Methods. The body part-based methods treat the skeleton as a set of connected rigid body segments (See Figure 4(b)) to model the human’s articulated system. Chaudhry et al. [192] divided the skeleton into many tiny parts, and then used bionic shape features to represent these body parts. Vemulapalli et al. [182] utilized the skeleton as points in a lie group to model the relative geometry between body parts. As shown in Figure 4(c), joint angles measure the geometric relationship of connected pairs of body parts, so the methods using joint angles can be classified as part-based methods as well. In [193], pairwise affinities between view-invariant joint angle features were used to represent actions. Ofli et al. [183] proposed to select the most informative representations based on the interpretable measures (e.g., the mean or variance of joint angle trajectories). [194] pointed out that the angle information is more discriminative than the joints’ normalized coordinates. In their further research [195], they introduced an extended formulation of the longest common sub-sequence algorithm to improve the recognition accuracy. Keceli and Can [196] utilized the angle representations as well, and they extracted features from both the angle and displacement information of the skeleton data, and utilized random forest and SVM to recognize actions.

3.2.2 Deep Learning Methods

Compared to hand-crafted feature-based methods, deep learning methods are more powerful for skeleton-based HAR. Most of the skeleton-based deep learning methods can be divided into three major categories: RNN, CNN, and Graph Neural Network (GNN) or GCN-based methods. Figures 5(a), 5(b), and 5(c) illustrate these three types of methods. TABLE 3 compares the performance of the skeleton-based deep learning HAR methods on the large-scale NTU RGB+D [178] and NTU RGB+D 120 [176] benchmark datasets.

RNN-Based Methods. RNNs are capable of learning the dependency and dynamic information within the sequential data, so the temporal context information within the skeleton sequences can be modeled by RNNs. As a successful variant of RNN, LSTM is able to reduce the possibility of gradient vanishing and exploding, and is suitable in modeling the long-term context dependence. Consequently, plenty of LSTM-based methods have achieved good results of HAR in long skeleton sequences.

In the past several years, different methods [197], [200], [244] have been proposed, which applied and adapted the

RNNs and LSTM networks for skeleton-based HAR. As one of the classic works, Du et al. [200] proposed an end-to-end hierarchical RNN that divides the human skeleton into five parts instead of inputting the skeleton in each frame as a whole. Then they separately fed the five parts into multiple bidirectional sub-nets. The representations were then hierarchically fused to generate high-level representations. Differential RNN (dRNN) [199] focused on the change in information gain caused by the salient motions between frames, and this change could be quantified by Derivative of States (DoS). Zhu et al. [197] introduced a novel mechanism for the LSTM network to achieve automatic co-occurrence mining, since co-occurrence intrinsically characterizes the actions. Sharoudy et al. [178] proposed Part-aware LSTM (P-LSTM) that introduces a mechanism to simulate the relations among different body parts inside the LSTM unit. Liu et al. [7], [245] proposed a Spatio-Temporal LSTM (ST-LSTM) network with trust gates, extending the RNN design to both the temporal and spatial domains. Specifically, they utilized the tree structure-based skeleton traversal method to further utilize the spatial information, and trust gates were used to deal with the noise and occlusion. In their further study, Liu et al. [204] proposed a new LSTM network termed Global Context-Aware Attention LSTM (GCA-LSTM), which is able to selectively focus on the informative joints using the global contextual information. The GCA-LSTM network uses two layers, where the first layer encodes the skeleton sequences and outputs a global context memory, while the second layer performs attention and outputs attention representations to refine the global context. Finally, the softmax layer classifies the actions. In [202], a new two-stream RNN structure for modeling both temporal dynamics and spatial configurations was proposed. Deep LSTM with spatio-temporal attention was proposed in [203], where a spatial attention sub-network and a temporal attention sub-network work jointly, under the main LSTM network. Lee et al. [205] proposed novel ensemble Temporal Sliding LSTM (TS-LSTM) networks composed of multiple parts, containing short-term, medium-term, and long-term TS-LSTM networks, respectively. IndRNN [208] not only addresses the problem of gradient vanishing and exploding issues, but also is faster than the original LSTM. Other LSTM-based methods include [201], [206], [246].

CNN-Based Methods. CNNs have achieved great success of image analysis, thanks to its superior capability in learning spatial information. But when facing the skeleton-based HAR tasks, how to model the temporal information becomes a challenge. Nevertheless, plenty of advanced approaches [210], [218] have been proposed, that convert the skeleton sequences into pseudo-images encoding both the spatial and temporal information. This means the spatial structure within each frame and the dynamic information between frames are simultaneously represented by the 2D pseudo-images, which can then be fed to normal CNNs for feature learning and action classification.

Hou et al. [210] and Wang et al. [211] respectively proposed the skeleton optical spectra and the Joint Trajectory Map (JTM), which both encode the spatio-temporal information of skeleton sequences into color texture images, and then adopt CNNs with classifiers to perform HAR tasks. As an extension of these works, the Joint Distance Map

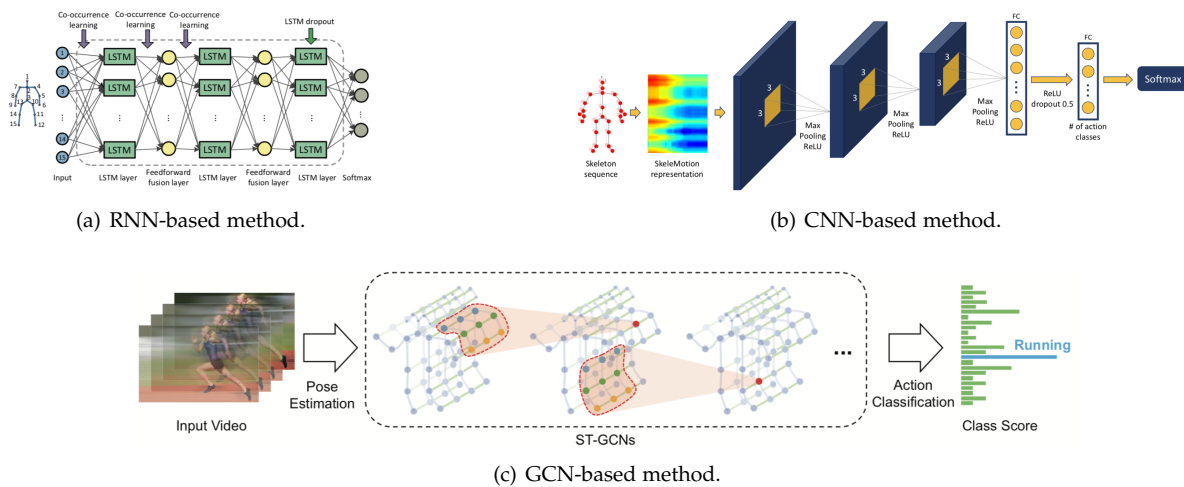


Fig. 5. An illustration of skeleton-based deep learning methods. (a) RNN and LSTM are able to model the temporal context information, and thus can be used for skeleton-based HAR. (b) Skeleton sequences can be converted to 2D pseudo-images that can be then fed to CNNs for feature learning. (c) The joint dependency structure naturally presents a graph structure, and thus GCN models are also suitable for this task. (a)-(c) are originally shown in [175], [197], [198].

(JDM) [214] is more robust to view variations. Ke et al. [215] transformed the skeleton sequence into three video ‘clips’ fed into CNN to get a compact representation. The output CNN representations are concatenated in a feature vector involving spatial and temporal information. Then a Multi-Task Learning Network (MTLN) is adopted for HAR. The idea of ‘clips’ is used in [218] as well. Kim and Reiter [212] used the Temporal CNN (TCN), which explicitly provides a type of interpretable spatio-temporal representations. In [219], residual one-dimensional CNN was used as the base network with four sub-nets ensembling together by late fusion to exploit different sources of features of the skeleton sequences. The four sub-nets are the two-stream model, the body-parted model, the attention model, and the frame-difference model, respectively. An end-to-end framework to learn co-occurrence features with a hierarchical methodology was proposed in [220]. Specifically, they learned the point-level features of each joint independently, and then utilized these features as a channel of the convolutional layer to learn hierarchical co-occurrence features. A two-stream framework was used to fuse motion features finally. Caetano et al. introduced SkeleMotion [198] and Tree Structure Reference Joints Image (TSRJI) [222] for a skeleton image representation as well. In [223], Skepxels were utilized as a basic building block to construct skeletal images that mainly encode the spatial information of human joint locations and velocities. Besides, Skepxels are to capture the micro-temporal relations, and Fourier Temporal Pyramids are employed to exploit the macro-temporal relations. Considering the spatial relationships among joints, Li et al. [224] used geometric algebra to represent the shape-motion. Some very recent methods [226], [227] also used CNNs for skeleton-based HAR.

Plenty of researches focus on addressing certain specific problems. For example, [214], [216], [225] focused on handling the viewpoint variation issue. Since features extracted from the skeleton are not always translation, scale, and rotation invariant, some methods [213], [217] were also

proposed for handling these issues. CNN architectures are complex resulting in high computation cost, and thus Yang et al. [221] proposed Double-feature Double-motion Network (DD-Net) to make the CNN-based recognition model run faster.

GNN or GCN-Based Methods. In recent years, due to the expressive power of graph structures, researches analyzing graphs with learning methods have received great attention [247], [248]. As shown in Figure 5(c), skeleton data is naturally in the form of graphs. And simply representing the skeleton data as a vector sequence processed by RNNs, or a 2D or 3D map processed by CNN, cannot fully model the complex spatio-temporal configurations and correlations of the body joints. This indicates topological graph representations can be more suitable for representing the skeleton data. As a result, in the domain of HAR, many GNN and GCN-based methods [175], [228] were proposed to treat the skeleton data as graph structures of edges and points, which focus on organizing the raw skeleton data into specific graphs.

GNN is a connection model capturing the dependence of graphs through message passing between nodes in the graphs. Si et al. [228] proposed a spatial reasoning network to capture high-level spatial structural information using GNN, and a temporal stack learning network was used to model the temporal dynamics. Shi et al. [229] represented the skeleton as a Directed Acyclic Graph (DAG) and utilized GNN to perform HAR. In [230], Dynamic Multi-scale GNN (DMGNN) utilized the multi-scale graphs to model the relations of the human body joints. Specifically, the DMGNN was developed based on the encoder-decoder framework. In DMGNN, multi-scale graphs are used to extract spatio-temporal features in the encoder, while the results are obtained by the graph-based gated recurrent unit in the decoder.

Very recently, GCN-based HAR is becoming a hot development direction. Yan et al. [175] exploited GCNs for skeleton-based HAR, as shown in Figure 5(c). They proposed Spatial-Temporal GCN (ST-GCN), which can auto-

TABLE 3

Performance comparison of skeleton-based deep learning HAR methods on NTU RGB+D and NTU RGB+D 120 datasets. ‘CS’, ‘CV’, and ‘CP’ respectively represent the cross-subject, cross-view, and cross-setup evaluation criteria.

	Methods	Reference	Year	Dataset			
				NTU RGB+D		NTU RGB+D 120	
				CS	CV	CS	CP
RNN-Based	dRNN	[199]	2015	-	-	-	-
	HBRNN	[200]	2015	59.1	64.0	-	-
	Co-occurrence LSTM	[197]	2016	-	-	-	-
	2 Layer P-LSTM	[178]	2016	62.9	70.3	25.5	26.3
	Trust Gate ST-LSTM	[7]	2016	69.2	77.7	58.2	60.9
	Zhang et al.	[201]	2017	70.3	82.4	-	-
	Two-stream RNN	[202]	2017	71.3	79.5	-	-
	STA-LSTM	[203]	2017	73.4	81.2	-	-
	GCA-LSTM	[204]	2017	74.4	82.8	58.3	59.2
	Ensemble TS-LSTM	[205]	2017	74.6	81.3	-	-
	VA-LSTM	[206]	2017	79.4	87.6	-	-
	MANs (DenseNet-161)	[207]	2018	82.7	93.2	-	-
	dense-IndRNN-aug	[208]	2019	86.7	93.7	-	-
CNN-Based	Du et al.	[209]	2015	-	-	-	-
	Hou et al.	[210]	2016	-	-	-	-
	JTM	[211]	2016	73.4	75.2	-	-
	Res-TCN	[212]	2017	74.3	83.1	-	-
	SkeletonNet	[213]	2017	75.9	81.2	-	-
	JDM	[214]	2017	76.2	82.3	-	-
	Clips+CNN+MTLN	[215]	2017	79.6	84.8	58.4	57.9
	Liu et al.	[216]	2017	80.0	87.2	60.3	63.2
	Li et al.	[217]	2017	85.0	92.3	-	-
	RotClips+MTCNN	[218]	2018	81.1	87.4	62.2	61.8
	Xu et al.	[219]	2018	84.8	91.2	-	-
	HCN	[220]	2018	86.5	91.1	-	-
	DD-Net	[221]	2019	-	-	-	-
	TSRJI	[222]	2019	73.3	80.3	67.9	62.8
	SkeleMotion	[198]	2019	76.5	84.7	67.7	66.9
	Skepxel	[223]	2019	81.3	89.2	-	-
	Li et al.	[224]	2019	82.9	90.0	-	-
	VA-fusion (aug.)	[225]	2019	89.4	95.0	-	-
	Banerjee et al.	[226]	2020	84.2	89.7	74.8	76.9
	Zhu et al.	[227]	2020	87.4	93.5	-	-
GNN-Based	SR-TSL	[228]	2018	84.8	92.4	-	-
	DGNN	[229]	2019	89.9	96.1	-	-
	DMGNN	[230]	2020	-	-	-	-
GCN-Based	ST-GCN	[175]	2018	81.5	88.3	-	-
	DPRL	[231]	2018	83.5	89.8	-	-
	motif-GCNs+non-local VTDB	[232]	2019	84.2	90.2	-	-
	BPLHM	[233]	2019	85.4	91.1	-	-
	AS-GCN	[234]	2019	86.8	94.2	-	-
	STGR-GCN	[235]	2019	86.9	92.3	-	-
	2s-AGCN	[236]	2019	88.5	95.1	-	-
	AGC-LSTM (Joint&Part)	[237]	2019	89.2	95.0	-	-
	2s-SDGCN	[238]	2019	89.6	95.7	-	-
	Advanced CA-GCN	[239]	2020	83.5	91.4	-	-
	SGN	[240]	2020	89.0	94.5	79.2	81.5
	GCN-NAS	[241]	2020	89.4	95.7	-	-
	4s Shift-GCN	[242]	2020	90.7	96.5	85.9	87.6
MS-G3D Net	[243]	2020	91.5	96.2	86.9	88.4	

matically learn both the spatial and temporal patterns from skeleton data. They estimated the pose from the input videos, and constructed the spatial-temporal graph, which is a good action representation method with strong generalization ability. But implicit joint correlations may be ignored. Thus Li et al. [234] proposed the Actional-Structural GCN (AS-GCN), which combines actional links and structural links into a generalized skeleton graph. Actional links are to capture action-specific latent dependencies, while structural links are to represent higher-order dependencies. To explore implicit joint correlations better, Peng et al. [241] is the first work that determines the GCN architecture with neural architecture search. Specifically, they enriched the

search space to implicitly capture joint correlations based on multiple dynamic graph substructures and higher-order connections with Chebyshev polynomial approximation. Besides, context information is utilized to model long-range dependencies as well [239].

Shi et al. [236] proposed a novel two-stream adaptive GCN (2s-AGCN) in which the topology of the graphs can be either uniformly or individually learned by the back-propagation algorithm, instead of setting manually. 2s-AGCN explicitly combines the second-order information (lengths and directions of human bones) of the skeleton with the first-order information (coordinates of the joints). Wu et al. [238] introduced a cross-domain spatial residual layer to

capture spatio-temporal information and a dense connection block to learn global information based on ST-GCN. In [235], the skeleton sequences were transformed as frame-wise skeleton and node trajectories, respectively, which were then fed into the spatial graph router and temporal graph router to get new skeleton-joint-connectivity graphs for further classification. High-level semantics of joints were introduced in [240]. The attention mechanism helps to extract discriminative information and global dependency [232], [237]. To decrease computation cost, a Shift-GCN was designed by Cheng et al. [242], which contains shift graph operations and lightweight point-wise convolutions, instead of using heavy regular graph convolutions. Liu et al. [243] integrated a disentangled multi-scale aggregation scheme and a unified spatial-temporal graph convolutional operator named G3D to achieve a powerful feature extractor termed as MS-G3D. Some other GCN-based methods include [231], [233].

In summary, the skeleton modality provides the body structure information, which is simple, efficient, and effective for representing human behaviors. Nevertheless, HAR using skeleton data still faces some challenges, due to the very sparse representation, the noisy skeleton information, the lack of shape information that can be important when handling human-object interactions. Hence, some of the existing works also focused on using depth maps for HAR, as discussed in the following section, since depth maps not only provide 3D geometric structure information but also keep the shape information.

3.3 DEPTH MODALITY

Depth maps refer to images where each pixel contains the distance information from a given viewpoint to the points in the scene. The depth modality, which is often robust to variations of color and texture, provides reliable 3D structure and geometric shape information of human subjects, and can be used for HAR.

The essence of constructing a depth map is converting the 3D data into a 2D image. Various techniques have been proposed to obtain depth images, which include active sensing sensors (e.g., Time-of-Flight and structured-light-based cameras) and passive sensing ones (e.g., stereo cameras) [39]. Active sensors emit radiation in the direction towards objects in the scene, and then measure the reflected energy from the objects to complete the collection of depth information. In contrast, passive sensors measure natural energy that is emitted or reflected by the objects in the scene. For example, as a type of passive sensor, stereo cameras usually have two or more lenses to simulate the binocular vision of human eyes to obtain depth images, where depth maps can be recovered by seeking image point correspondences across stereo pairs [249]. Compared to many active sensors, such as Microsoft Kinect and Intel RealSense3D, passive sensors can provide higher resolution of depth maps, which, however, are often computationally expensive and sensitive to ambient light, and moreover, they can be inefficient in texture-less regions or highly textured regions with repetitive patterns.

In this section, we review methods that use depth maps for HAR. In particular, both the hand-crafted feature-based

and deep learning HAR methods using depth modality are reviewed. Note that only a few works used depth maps captured by stereo cameras for HAR [250], [251], while most of the existing methods [252], [253] focus on using depth videos captured by active depth sensors to recognize human actions, thanks to the development of consumer-available and reliable active sensors like Kinect.

3.3.1 Hand-crafted Feature-Based Methods

In [254], an action graph was proposed to model the temporal dynamics of the action instance, and a bag of 3D points is utilized to characterize postures. The most significant limitations of this method are its computational complexity and the lack of spatial context information. Thus, Space-Time Occupancy Patterns (STOP) [255] representing the depth sequence in a 4D space-time grid was proposed, which preserves spatial and temporal contextual information between space-time cells. Depth-based methods are generally sensitive to noise and occlusion. For this, researchers have designed robust features to address this problem, which include Random Occupancy Pattern (ROP) features extracted from depth images [256] and STIPs extracted from depth videos (called DSTIP) [257]. Lu et al. [258] also designed range-sample features that are binary and invariant w.r.t scale, viewpoint, and background variations. Besides, Rahmani et al. [252] also proposed a depth-based HAR algorithm, which is robust to occlusions. Specifically, the algorithm of [252] combines depth features (4D depth and depth gradient histograms) and 3D joint position estimations (local joint displacement histograms and joint movement occupancy volume features), and uses random decision forests for feature pruning and classification.

Some methods [259], [260] for HAR from depth map videos were developed based on projected depth maps (i.e., projecting depth data to several orthogonal 2D planes). Yang et al. [259] introduced Depth Motion Map (DMM) for HAR by projecting depth maps onto three orthogonal Cartesian planes, corresponding to front, side, and top viewpoints, and then computing motion energy between consecutive depth maps. Finally, HOG descriptors were computed from the DMM of each viewpoint to represent actions. Thanks to the success of DMM, several other HAR methods [260], [261], [262] were also proposed based on it. Chen et al. [262] employed DMMs to capture motion cues, and utilized Local Binary Patterns (LBPs) to gain feature representations. Chen and Guo [260] also presented a framework, called TriViews, that projects depth maps onto three orthogonal planes and evaluates the performance of different features such as STIPs, dense trajectory shapes, and dense trajectory motion boundary histograms. However, this type of method is extremely dependent on the viewpoint, and generally needs much computation due to the holistic representations, which constraints their applicability in handling challenging scenarios.

The surface normal can provide much shape and structure information of the subjects. Hence, Oreifej and Liu [263] presented a novel descriptor termed as HON4D applying the surface normal for depth-based HAR. Since the calculation of the HON4D descriptor needs to be performed on the entire video sequence, this method needs to perform temporal and spatial alignment first. As an extension work of

HON4D, Yang and Tian [253] utilized depth map sequences to construct Super Normal Vector (SNV) features, which can capture local motion and geometric information at the same time. Specifically, they grouped hyper-surface normals from a depth sub-volume into polynormals, then aggregated low-level polynormals into the SNV, and finally applied spatial-temporal pyramids.

3.3.2 Deep Learning Methods

Compared to the aforementioned hand-crafted feature-based methods, deep learning methods [8], [264] are more powerful and achieve better performance for HAR from depth maps. An end-to-end HAR learning framework, utilizing weighted hierarchical DMMs based on three CNNs via score fusion, was proposed in [265]. As DMMs are not able to capture detailed temporal information, local spatio-temporal descriptors considering both the shape discrimination and action speed variations were designed in [266]. In [264], depth sequences were represented with three pairs of structured dynamic images at the body, part, and joint levels by utilizing bi-directional rank pooling [267], and then Spatially Structured Dynamic Depth Images (S²DDI) were constructed and fed into CNNs for fine-grained HAR. The performance of this method was further improved in [268] by introducing three representations of depth maps, including dynamic depth images (DDIs), dynamic depth normal images (DDNIs), and dynamic depth motion normal images (DDMNIs).

Besides, Zhu and Newsam [269] introduced Depth2Action using two-stream and C3D networks for HAR. Rahmani et al. [8] transferred the human data obtained from different views to a view-invariant high-level space to address the view-invariant HAR problem. Specifically, they utilized a CNN model to learn the view-invariant human pose model and Fourier Temporal Pyramids to model the temporal action variations. To obtain much multi-view training data, synthetic data was generated by fitting synthetic 3D human models to the real motion capture data, and rendering the human data from various viewpoints. In [270], multi-view dynamic images were extracted through multi-view projection in depth videos for action characterization. An end-to-end 3D Fully CNN (3D-FCNN) was introduced in [271], which can automatically encode spatio-temporal information without pre-processing. In their subsequent work [272], a variant of LSTM, named stateful ConvLSTM, was further introduced to address the problem of memory limitation during video processing, which can be used to perform HAR from long and complex videos effectively.

In general, the depth modality provides geometric shape information that is useful for HAR. However, the depth data is often not used alone due to the lack of appearance information that can also be helpful for HAR in some scenarios. Thus, many works focused on fusing depth information with other data modalities for enhanced HAR. More details can be found in Section 4.

3.4 INFRARED SEQUENCE MODALITY

Infrared sensors usually do not rely on external ambient light, and are particularly suitable for HAR at night. Infrared

technologies can be divided into active and passive ones. Some infrared sensors, such as Kinect, rely on active infrared technology, which emit infrared rays and utilize target reflection rays to perceive objects in the scene. In contrast, thermal sensors relying on passive infrared technology do not emit infrared rays. Instead, they work by detecting rays (i.e., heat energy) emitted from targets.

Traditional hand-crafted feature-based methods [273], [274] exploiting infrared data have been used for gait recognition [273], [275] and night HAR [274], [276]. Recently, plenty of deep learning architectures [277], [278] have also been proposed for infrared data-based HAR. In [277], a framework using convolutional layers for modeling spatial information and LSTM layers for modeling temporal dependencies was designed for HAR. Shah et al. [278] used 3D CNNs and achieved real-time HAR in infrared data. In [279], the 3D CNN used optical flow information computed from infrared data as input for HAR. HAR using CNNs over infrared data was studied in [280] as well.

As optical flow maps encode motion information that can be important for HAR, multi-stream deep learning architectures (containing optical flow streams) [9] have been widely used for infrared data-based HAR. Infrared and optical flow volumes were fed to a two-stream 3D CNN framework for HAR in [9]. Low-resolution thermal images and optical flow maps were combined in a two-stream network in [281]. Liu et al. [282] introduced an Optical-Flow Stacked Difference Image (OFSDI) as a global temporal representation, and then fed optical flow, OF-MHI, and OFSDI into three-stream CNNs for HAR. Imran and Raman [283] built a four-stream deep framework based on CNN and LSTM, using Stacked Dense Flow Difference Images (SDFDIs) [284] and Stacked Saliency Difference Images (SSDIs). Mehta et al. [285] presented a novel adversarial network consisting of two-channel 3D convolutional auto-encoders, which took thermal data and optical flow as inputs for fall detection.

In all, the infrared data has been widely used for HAR, especially for night HAR, thanks to its workability in dark environments. However, infrared images may suffer from relatively low contrast and low signal-to-noise ratio, making it challenging for robust HAR in some scenarios.

3.5 POINT CLOUD MODALITY

Point cloud data is composed of a massive collection of points that express the spatial distribution and surface characteristics of the target under a spatial reference system. There are two main ways to obtain 3D point cloud data, namely, (1) using 3D sensors, such as LiDAR and Kinect, and (2) using image-based 3D reconstruction. As a 3D data modality, point cloud has great power to represent spatial silhouettes and 3D geometric shapes of the subjects, and can be used for HAR.

Rusu et al. [286] represented action shapes as 3D point clouds using 3D point-based geometry methods, and then computed feature histogram descriptors to recognize actions. The framework of clouds of space-time interest points was introduced in [287] for action classification. Munaro et al. [288] proposed a 3D grid-based descriptor encoding the whole person motion from colored point clouds as well as real-time 3D motion flow estimation for HAR.

Rahmani et al. [289], [290] integrated the local Histogram of Oriented Principal Components (HOPC) descriptors with Spatio-Temporal Key-Points (STKPs) detection for cross-view HAR. Similar to the STOP descriptors [255], the descriptors designed in [291] captured a point cloud structure through a modified 3D regular grid with corresponding cell space occupancy information, which were then used for HAR. Recently, Wang et al. [10] proposed a 3D motion representation, called 3D Dynamic Voxel (3DV), to encode 3D action information into a voxel set with temporal rank pooling. The voxel representation was then abstracted and passed through the PointNet++ model [292] for 3D HAR.

In all, the point cloud modality can effectively capture the 3D shapes and silhouettes of the subjects, and can be used for HAR, and generally, 3D point cloud-based HAR methods can be insensitive to viewpoint variations, since viewpoint normalization can be conveniently performed by rotating the point cloud in 3D space.

3.6 EVENT STREAM MODALITY

Event cameras, also known as neuromorphic cameras or dynamic-vision sensors, which can capture illumination changes and produce asynchronous events independently for each pixel [293], have received lots of attention recently. Different from conventional video cameras capturing the entire image arrays, event cameras only respond to changes in the visual scene. Taking a high-speed object as an example, traditional RGB cameras may not be able to capture enough information of it, due to the low frame rate and motion blur. However, this issue can be significantly mitigated when using event cameras that operate at extremely high frequencies, generating events at a μs temporal scale [293]. Besides, event cameras have some other characteristics, such as high dynamic range, low latency, low power consumption, and no motion blur, which make them suitable for HAR. Particularly, event cameras are able to effectively filter out background information and keep foreground movement only, avoiding considerable redundancy in visual information. However, the information obtained with event cameras is generally spatio-temporally sparse, and asynchronous. Common event cameras include the Dynamic Vision Sensor (DVS) [294] and the Dynamic and Active-pixel Vision Sensor (DAVIS) [295], etc.

The output data of event cameras is highly different from that of conventional RGB cameras, as shown in Table 1. Thus, some of the existing methods [296] mainly focused on designing event aggregation strategies converting the asynchronous output of the event camera into synchronous visual frames, which can then be processed with conventional computer vision techniques. While hand-crafted feature-based methods [296], [297] have been proposed, deep learning methods are more popularly used recently. Ghosh et al. [298] introduced spatio-temporal filtering in the spike-event domain, where the raw event data was convolved with 3D spatio-temporal filters to generate multiple filtered channels, as the input of a CNN followed by a classifier. However, it remains to be seen for static recognition tasks. Innocenti et al. [293] proposed Temporal Binary Representation (TBR), where events were first stacked together into intermediate binary representations,

which were then losslessly grouped into a single frame via a binary to decimal conversion, interpreted by deep learning models finally. Huang et al. [299] utilized timestamp image encoding, to encode the event data sequence into frame-based representations for HAR. Bi et al. [300] proposed a compact graph representation for end-to-end learning with Residual-Graph CNN (RG-CNN). Event cameras have also been used for gesture recognition in [301], which achieved promising results. However, since the size of the frame to be processed in these methods is basically larger than the original Neuromorphic Vision Stream (NVS), the advantages of event cameras are diluted.

Therefore, different from the aforementioned methods, some other methods [302], [303], [304], [305], directly using the event stream as the input of networks, have also been proposed. George et al. [304] utilized Spiking Neural Networks (SNNs) for event stream-based HAR. The works in [302], [303] treated the event stream as the 3D point cloud, which was then fed into deep networks for gesture recognition. Chadha et al. [305] embedded the PIX2NVS emulator [11] (converting pixel domain video frames to neuromorphic spike events) into a teacher-student framework based on knowledge distillation, which transferred knowledge from a pre-trained optical flow teacher network to the Neuromorphic Vision Sensing (NVS) student network. After training, the emulator component of the framework was replaced with an NVS camera for HAR without using optical flow, achieving promising recognition performance and low computation complexity.

In general, the event stream modality is an emerging modality for HAR, and has received great attention in the past few years. Processing event data is computationally cheap, and the captured frames usually do not contain background information, which can be helpful for action understanding. However, the event stream data generally cannot be effectively and directly processed using conventional video analysis techniques, and thus effectively and directly utilizing the asynchronous event stream for HAR is still a challenging research problem.

3.7 AUDIO MODALITY

The audio signal is the form of sound, mainly existing in videos for HAR. Due to the synchronization between visual and audio streams, the audio data can be used to locate actions to save human labeling efforts and decrease computational cost. Audio modality is often used as complement information of visual modalities for HAR, and thus most of the existing audio-based methods [17], [306] focus on using multi-modal deep learning technique, which are discussed in 4.

Several hand-crafted feature-based methods [56], [307] were proposed for HAR with audio signal. More recently, plenty of methods [308], [309], [310], [311] that utilized multi-stream deep learning architectures were proposed, in which the visual and audio modalities were fed into CNNs to perform HAR tasks via a fusion strategy. Hori et al. [306] integrated the temporal attention mechanism into an RNN encoder-decoder model to fuse information across RGB and audio modalities, resulting in a reliable HAR model. In the work of [17], two different architectures, including Temporal

Binding Network (TBN) and Temporal Segment Network (TSN) [106], were evaluated. Specifically, the RGB, flow, and audio information were fused with a mid-level fusion technique and were trained jointly in TBN, while the data was trained independently in TSN with an additional audio stream performing late fusion. Gao et al. [12] utilized audio as a clip-level preview tool in untrimmed videos for efficient HAR.

In general, using audio modality alone is not a popular scheme of HAR, since the audio signal does not contain enough information for accurate HAR. Nevertheless, the audio modality can serve as complementary information for more reliable and efficient HAR, as shown by the existing works [12], [306].

3.8 ACCELERATION MODALITY

Acceleration signals obtained from accelerometers have been used for HAR [312], thanks to the robustness against occlusion, view, lighting, and background variations, etc. Specifically, a triaxial accelerometer can return an estimation of acceleration along the x , y , and z axes, that can be used to perform human activity analysis [313]. As for the feasibility of the acceleration signals for HAR, although the size and proportion of the human body vary from person to person, people generally have similar qualitative ways to perform an action, so the acceleration signals do not have obvious intra-class variations for the same action. HAR using acceleration signals can generally achieve high accuracy, and thus has been adopted for remote monitoring systems [314], [315] while taking care of privacy issues.

Plenty of traditional hand-crafted feature-based approaches [57], [312], [313], [314], [316], [317], [318], [319], [320] have been proposed for HAR using acceleration data. These methods placed several accelerometers on different parts of the human body to obtain raw acceleration signals. The signals were then pre-processed by removing the noise or performing segmentation using window-overlapping techniques. Finally, descriptive features were extracted by applying different techniques, such as Principal Component Analysis (PCA) and wavelet transform, for HAR. The combination of accelerometers and other sensors has also been adopted for HAR [315], [321], [322].

Deep learning networks have been widely applied as well, since they can learn discriminative features. Zeng et al. [13] captured local dependencies and scale-invariant features of acceleration signals by PCA and Restricted Boltzmann Machine (RBM), etc., and these features were then fed to CNNs to produce the classification results. In the work of [323], the signal sequences of accelerometers and gyroscopes were assembled into an activity image, which was then fed into a CNN. Ordonez and Roggen [324] combined convolutional and LSTM units into a framework explicitly capturing the temporal dynamics, for HAR. In the work of [325], CNN was augmented with statistical features embracing global properties from acceleration sequences for recognition. Fan et al. [326] adopted an algorithm-hardware co-design scheme to decrease computational cost.

In general, the acceleration modality can be utilized for fine-grained HAR, and has been used for action monitoring, especially for eldercare thanks to its privacy-protecting

characteristic. However, the subject needs to carry wearable sensors that are often cumbersome and disturbing. In addition, the place of sensors can also affect the performance of HAR.

3.9 RADAR MODALITY

Radars are active sensing systems that transmit electromagnetic waves and receive returned waves from targets. There are some advantages of using spectrograms obtained from radars for HAR, which include the robustness to variations of illumination and weather conditions, privacy protecting during HAR, and capability of through-wall HAR [49]. Continuous-wave radars, such as Doppler radars [327] and Frequency Modulated Continuous Wave (FMCW) radars [328], are most often chosen for HAR. Specifically, continuous-wave radars detect the radial velocity of body parts (and thus are hard to be used to recognize non-cooperative actions performed along the tangent direction), and the frequency changes according to the distance, which is known as Doppler shift. The micro-Doppler signatures generated by the micro-motion of the radar target contain the motion and structure information of the target, which thus can be used for HAR. As for the FMCW radars, they can measure the distances of the targets as well.

Some hand-crafted feature-based HAR methods using radar data have been designed in the works of [329], [330], [331]. Plenty of deep learning-based methods [14], [332] have also been proposed recently. The works in [14], [332], [333], [334] directly fed raw micro-Doppler spectrogram images to CNNs for HAR, while [335] designed a three-layer deep convolutional auto-encoder, combining the advantages of CNNs and auto-encoders for radar-based HAR. Vandermissen et al. [336] computed the micro-Doppler signatures from the recorded raw signals, and then did noise reducing and segmentation pre-processing. Finally, they trained a CNN model to get the recognition result. LSTM networks were utilized for radar-based HAR as well [337], [338]. Wang et al. [337] performed the logarithm operation and normalization on spectrograms of raw radar data. Then the input was fed into the stacked RNN network for action classification.

In general, the characteristics and advantages of the radar modality make it suitable to be used for HAR in some scenarios, but the radars are relatively expensive. Though HAR using radar data has achieved satisfactory results on some datasets, there is still plenty of room for the development of the radar-based methods, and the work of [49] also pointed out some future directions in this area, such as handling more complex actions in real-world scenarios with the radar data.

3.10 WIFI MODALITY

WiFi has been considered as one of the most common indoor wireless signal types nowadays [339]. Since human bodies are good reflectors of wireless signals, WiFi signals can be utilized for HAR. There are some advantages of using the WiFi modality for action analysis, thanks to the convenience, simplicity, privacy protection, and low cost of the WiFi signals and devices. However, in WiFi-based HAR, the spatial range of the action performing is not large, and

the recognition accuracy is also limited. Specifically, most of the existing WiFi-based HAR methods [15], [340] focused on using the Channel State Information (CSI) to conduct action recognition. CSI is the fine-grained information computed from the raw WiFi signals, and the WiFi signals reflected by a person, who performs an action, usually generate unique variations in the CSI on the WiFi receiver.

E-eyes system [15] is a classic work that utilized CSI histograms as fingerprints to perform daily activity recognition. In the works of [58], [340], a CSI-based human activity recognition and monitoring system was proposed. The system consists of two models, namely, a CSI-speed model and a CSI-activity model, that can quantitatively correlate CSI dynamics and human activities. Wang et al. [341] proposed WifiU, generating spectrograms from CSI measurements and extracting features for capturing fine-grained activity patterns based on commercial off-the-shelf WiFi devices. The work of [342] used specialized directional antennas to obtain CSI variations caused by lip movements. Duan et al. [343] handled driver activity recognition based on WiFi CSI. Besides, WiFi signals have also been used for fall detection [344].

Deep learning networks [339] have received much attention as well. In the work of [345], the WiFi-based sample-level HAR task was handled, which is different from the past series-level recognition problem. More specifically, every WiFi distortion sample in the series was categorized into one action, whereas series-level HAR generally categorizes the complete distortion series into one action. A deep model, called Temporal Unet, was introduced by [345], and the CSI was used as the time-serial WiFi distortion that can be fed into the network for recognition tasks. Zou et al. [339] designed an architecture named WiVi, taking RGB and WiFi data as inputs of the C3D and CNN models, and then performed multi-modal fusion for classification.

In general, thanks to the advantages (e.g., convenience) of the WiFi modality, it can be used for HAR in some scenarios. However, there are still some challenges that need to be addressed, such as more effectively using the CSI phase and amplitude information, and improving the robustness when handling dynamic environments, etc.

3.11 OTHER MODALITIES

Apart from the modalities mentioned above, other sensor-based modalities, such as pressure [346], orientation [346], gyroscope [346], [347], radio-frequency (RF) [348], [349], Piezoelectric Energy Harvester (PEH) [350], [351], and electromyography (EMG) [352], etc., have been applied for HAR as well. Moreover, recently, Nagrani et al. [353] introduced the speech modality, neither visual nor sensor modalities, for action recognition, and they trained a Speech2Action model from literary screenplays to predict action labels from transcribed speech segments.

4 MULTI-MODALITY

In real life, humans often perceive the environment in a multi-modality cognition way. Similarly, multi-modality machine learning can be used for HAR as well. Specifically, multi-modality machine learning is a modeling approach

aiming to process and relate the information from multiple modalities [354]. Aggregating the advantages and capabilities of various data modalities, multi-modality machine learning can often provide high accuracy and robustness of HAR. There are two main types of multi-modality learning methods, namely, fusion and co-learning. Fusion refers to fusing the information from two or more modalities for training and inference, while co-learning refers to transferring knowledge among different data modalities.

4.1 FUSION

As introduced in Section 3, different modalities can have different strengths. Thus it becomes a natural choice to take advantage of the complementary strengths of different data modalities via fusion, so as to achieve enhanced HAR performance. There are two widely used multi-modality fusion schemes in HAR, namely, late fusion and early fusion. Generally, late fusion [362], [363] is decision-based, which integrates the decisions that are separately made based on different modalities, to produce the final classification result. As it is usually very convenient and effective to directly fuse the classification results (confidence scores) obtained based on different modalities, late fusion has been quite popularly adopted for HAR. Meanwhile, early fusion [52], [364] is generally feature-based, and it combines the features of different modalities to yield aggregated features that are often very discriminative and powerful and can then be used for HAR. Note that in some works [7], other fusion methods, such as intermediate feature fusion [7], have also been exploited, and since they perform feature-based fusion as well, here we simply group them to early fusion.

Table 4 gives the results of multi-modality fusion-based HAR methods on the MSR-Action3D [254], MSRDailyActivity3D [184], UTD-MHAD [347], and NTU RGB+D [178] benchmark datasets.

4.1.1 Fusion of Visual Modalities

With the emergence of low-cost RGB-D cameras, many multi-modality datasets [178], [184] have been created by the community, and consequently, plenty of multi-modality fusion-based HAR methods appeared [52], [364]. Most of these methods focused on the fusion of visual modalities, such as RGB, depth, and skeleton data, which are reviewed below.

Fusion of RGB and Depth Modalities. The RGB and depth data respectively capture rich appearance information and 3D shape information, that are complementary and can be used for HAR. As a result, different methods [52], [355] have been proposed to exploit the fusion of these two modalities for more reliable action recognition. Ni et al. [52] introduced two fusion methods naturally combining RGB and depth features, including Depth-Layered Multi-Channel STIPs (DLMC-STIPs) and 3D-MHIs, for HAR. In the work of [355], HOG and HOF descriptors from RGB data, and Local Depth Patterns (LDP) features from depth data were fused for activity classification. Liu and Shao [356] proposed a Restricted Graph-based Genetic Programming (RGGP) approach, simultaneously extracting and fusing the RGB and depth information, and in this method, a group of 3D operators were used to evolve the individual program

TABLE 4

Performance comparison of multi-modality fusion HAR methods on MSR-Action3D (M1), MSRDailyActivity3D (M2), UTD-MHAD (U) and NTU RGB+D (N) benchmark datasets. Notation: S: Skeleton, D: Depth, IR: Infrared sequence, PC: Point Cloud, Acc: Acceleration, Gyr: Gyroscope.

Method	Reference	Year	Modality	Deep Network	Fusion	Dataset				
						M1	M2	U	N	
									CS	CV
DLMC-STIPs	[52]	2011	RGB,D	None	Early	-	-	-	-	-
3D-MHIs	[52]	2011	RGB,D	None	Early	-	-	-	-	-
Zhao et al.	[355]	2012	RGB,D	None	Early	-	-	-	-	-
RGGP	[356]	2013	RGB,D	None	Early	-	85.6	-	-	-
BHIM	[357]	2015	RGB,D	None	Early	-	86.9	-	-	-
Structured MMHIM-2	[358]	2017	RGB,D	None	Early	-	89.4	-	-	-
Imran et al.	[359]	2016	RGB,D	CNN	Late	-	-	91.2	-	-
SFAM	[360]	2017	RGB,D	CNN	Late	-	-	-	-	-
c-ConvNet	[18]	2018	RGB,D	CNN	Late	-	-	-	86.4	89.1
GM-VAR	[361]	2019	RGB,D	GAN	Early	-	-	-	-	-
Dhiman et al.	[362]	2020	RGB,D	CNN,LSTM	Late	-	-	-	79.4	84.1
Wang et al.	[363]	2020	RGB,D	CNN,RNN	Late	-	-	-	89.5	91.7
SSFF	[364]	2014	RGB,S	None	Early	-	81.9	-	-	-
Franco et al.	[365]	2020	RGB,S	None	Late	-	-	-	-	-
ST-LSTM	[7]	2017	RGB,S	LSTM	Early	-	-	-	73.2	80.6
DSSCA-SSLM	[366]	2017	RGB,S	Autoencoder	Early	-	97.5	-	74.9	-
Chain-MS	[367]	2017	RGB,S	CNN	Late	-	-	-	80.8	-
Zhao et al.	[368]	2017	RGB,S	CNN,RNN	Early	-	-	-	83.7	93.7
Baradel et al.	[369]	2017	RGB,S	CNN,LSTM	Late	-	90.0	-	84.8	90.6
Liu et al.	[370]	2018	RGB,S	LSTM	Late	-	-	-	-	-
SI-MM	[371]	2018	RGB,S	CNN,LSTM	Late	-	91.9	-	92.6	97.9
DS+DCP+DDP+Joule+SVM	[372]	2015	RGB,S,D	None	-	-	95.0	-	-	-
Ye et al.	[373]	2015	RGB,S,D,PC	None	Late	90.4	-	-	-	-
MMHIM+Skeleton	[358]	2017	RGB,S,D	None	Early	-	95.6	-	-	-
CMFL	[374]	2019	RGB,S,D	None	Early	-	95.6	92.1	72.3	78.6
Chaarouai et al.	[375]	2013	S,D	None	Early	91.8	-	-	-	-
DCSF+Joint	[257]	2013	S,D	None	Early	-	88.2	-	-	-
Zhu et al.	[179]	2013	S,D	None	Early	94.3	-	-	-	-
JAS+HOG ²	[193]	2013	S,D	None	Early	94.8	-	-	-	-
Rahmani et al.	[252]	2014	S,D	None	Early	88.8	74.5	-	-	-
Althloothi et al.	[376]	2014	S,D	None	Early	-	93.1	-	-	-
MMMP	[377]	2015	S,D	None	Early	98.2	91.3	-	-	-
Jala et al.	[378]	2017	S,D	HMM	Early	93.3	94.1	-	-	-
PRNN	[379]	2017	S,D	CNN,RNN	-	94.9	-	-	-	-
Rahmani et al.	[380]	2017	S,D	CNN	Early	-	-	-	75.2	83.1
Kamel et al.	[381]	2018	S,D	CNN	Late	94.5	88.1	-	-	-
3DSTCNN	[382]	2019	S,D	CNN	Late	94.2	-	95.3	-	-
Chen et al.	[383]	2014	D,Acc	None	Early,Late	-	-	-	-	-
Chen et al.	[384]	2015	S,D,Acc	None	Late	-	-	97.2	-	-
Zou et al.	[385]	2017	RGB,D,Acc	None	Early	-	-	-	-	-
MHCCA	[386]	2018	RGB,S,D,Acc	None	Early	93.5 (S+D)	-	96.1	-	-
JMHC	[387]	2019	S,D,Acc	None	Late	-	-	94.9	-	-
Ehatisham et al.	[388]	2019	RGB,Acc,Gyr	None	Early	-	-	97.6	-	-
DCNN	[323]	2015	Acc,Gyr	CNN	Early	-	-	-	-	-
DeepConvLSTM	[324]	2016	Acc,Gyr	CNN,LSTM	Late	-	-	-	-	-
WiVi	[339]	2019	RGB,WiFi	CNN	Late	-	-	-	-	-
Memmesheimer et al.	[389]	2020	S,WiFi,etc.	CNN	Early	-	-	93.3	-	-
FUSION-CPA	[390]	2020	S,IR	CNN	Early	-	-	-	91.6	94.5
Zou et al.	[391]	2020	Acc,Gyr	CNN,LSTM	Late	-	-	-	-	-
Imran et al.	[284]	2020	RGB,S,Gyr	CNN,RNN	Late	-	-	97.9	-	-

to obtain discriminative representations. Bi-linear Heterogeneous Information Machine (BHIM) [357] and Max-Margin Heterogeneous Information Machine (MMHIM) [358] were also used to compress and project heterogeneous data to a learned shared space. Besides, they utilized feature matrices, instead of feature vectors, to represent actions, so as to keep inherent spatio-temporal structural information within the features.

Deep learning architectures [359], [362] have also been used for RGB and depth data fusion-based HAR. In the work of [359], a four-stream deep CNN architecture was designed, which was fed with three DMMs from the front, side, and top views generated from depth data, and MHI generated from RGB data. Dhiman et al. [362] designed a two-stream network composed of a motion stream and a Spatial-Temporal Dynamic (STD) stream. In the work of

[18], a c-ConvNet was cooperatively trained on RGB Visual Dynamic Image (VDI) features and Depth Dynamic Images (DDI) features. Specifically, the c-ConvNet cooperatively exploited the information in RGB VDIs and DDIs by jointly optimizing a ranking loss and a softmax loss. Wang et al. [360] proposed a representation method, called Scene Flow to Action Map (SFAM), extracting features from depth and RGB modalities as a joint entity for HAR. In the work of [361], a Generative Multi-View Action Recognition (GM-VAR) framework was introduced, which generated one view conditioned on the other views to make HAR more robust to cross-view settings. In the work of [363], a hybrid network of CNN and RNN was proposed, where weighted dynamic images were fed into CNNs, while RGB and depth sequences were fed into 3D ConvLSTMs to extract features. Then a canonical correlation analysis was applied to fuse

these features.

Fusion of Skeleton and Depth Modalities. The skeleton data has been shown to be a succinct yet informative representation for human behavior analysis [392], which, however, is a very sparse representation without encoding shape information of the human body and the interacted objects. Besides, the skeleton data is often noisy, limiting the performance of HAR when using skeleton data only [7]. Meanwhile, the depth maps provide discriminative 3D shape and silhouette information that can be helpful for HAR. Therefore, many methods [193], [257] have attempted to fuse the skeleton and depth information for more accurate HAR. The body pose and shape information based on silhouettes were fused through feature concatenation in [375]. Depth Cuboid Similarity Features (DCSFs) were concatenated with the joint position features in [257]. Ohn-Bar and Trivedi [193] proposed two descriptors extracted from skeleton and depth sequences, which include Joint Angle Similarity (JAS) and HOG² features. A bag-of-words scheme and a SVM classifier were further used for HAR. In the work of [376], shape features extracted via spherical harmonics representations and motion information of the 3D joint positions were fused by Multiple Kernel Learning (MKL), which is a model-based fusion strategy. In the work of [179], features were fused based on the random decision forests method. Shahroudy et al. [377] employed a heterogeneous set of skeleton features (joint trajectories) and depth features (local occupancy patterns and histograms of oriented 4D normals) for HAR.

As for deep learning-based approaches, Shi and Kim [379] proposed an RNN architecture driven by Privileged Information (PI), and they pre-trained an embedded encoder taking depth maps and skeleton as input. Then a multi-task loss was applied to exploit the PI in the regression term as a secondary task. Besides, a bridging matrix was also defined to discover the latent PI at the final refining step. Jalal et al. [378] extracted multi-fused features consisting of four sets of joint features from skeleton sequences and one set of body shape features from depth sequences, and then adopted HMM for recognition. In the work of [380], an end-to-end learning framework effectively combining representations from skeleton data and depth images was introduced. CNNs were used in [381] to take in Depth Motion Images (DMIs) and Moving Joint Descriptors (MJDs) for HAR via score fusion. The work of [382] utilized two 3D Space-Time CNN (3DSTCNN) streams taking raw depth data and depth motion map as input, as well as a manifold representation stream taking 3D skeleton as input, for action classification.

Fusion of RGB and Skeleton Modalities. The appearance information provided by RGB data, and body posture and joint motion information provided by skeleton sequences, are complementary and useful for activity analysis. Thus RGB and skeleton data fusion-based approaches [7], [366] have also been introduced for HAR. In the work of [364], the hierarchical bag-of-words feature fusion technique based on structured sparsity learning was proposed to fuse features from the RGB and skeleton data. Franco et al. [365] utilized HOG descriptors derived from the RGB frames to highlight the temporal evolution of actions, together with skeleton information to capture body postures.

Besides, some deep learning-based methods [368], [369] have also been proposed. The two-stream deep network was utilized in [368], where the RNN stream and the CNN stream were fed with skeleton and RGB data, respectively. They further evaluated both feature-based fusion and decision-based fusion, and found the former achieved a superior result. Baradel et al. [369] fused a model based on pose sub-sequences and a spatio-temporal attention model on RGB data conditioned on pose features for HAR. Chained Multi-Stream (Chain-MS) networks [367] integrated multiple cues (pose, optical flow, and RGB) sequentially via a Markov chain model. Liu et al. [7] studied early fusion and late fusion, together with the newly proposed feature fusion strategy above the spatio-temporal LSTM network [7] for action analysis. Shahroudy et al. [366] presented a method of hierarchical shared-specific component factorization. They focused on studying the correlation between modalities, and factorizing them into their correlated and independent components. Then a structured sparsity-based classifier was utilized for feature fusion. Liu et al. [370] proposed a two-stream multi-modality multi-task RNN. Song et al. [371] proposed a Skeleton-Indexed Multi-Modality (SI-MM) feature learning framework containing a skeleton-indexed transform layer and a part-aggregated pooling layer, where the skeleton-indexed transform explicitly captured local details with high resolution, while the part-aggregated pooling layer was to adapt to different dimension skeleton-indexed features.

Other Fusion Methods. Besides fusing two data modalities, some methods [372], [374] have explored fusing three or more modalities to further enhance the robustness of HAR. As different features may share similar hidden structures, a joint heterogeneous feature learning method was introduced in [372] to explore the shared and feature-specific components based on RGB, depth, and 3D skeleton data. Since some fusion-based methods simply concatenated the features and ignored their latent connections, Kong et al. [374] proposed a Collaborative Multi-modal Feature Learning (CMFL) model, where RGB, skeleton, and depth data were factorized to learn shared features to discover their latent connections.

Moreover, besides fusing the RGB, depth, and skeleton information, some other methods [373] have also attempted to fuse other visual modalities, such as point cloud data, for HAR as well. For example, the point cloud data was fused with other visual modalities in [373], where a multi-modal feature fusion method was proposed to exploit different discriminative capabilities of the features extracted from multiple modalities.

4.1.2 Fusion of Visual and Sensor Modalities

Visual and sensor modalities can also be fused to leverage their complementary discriminative capabilities for better HAR accuracy and higher robustness. Chen et al. [383] fused depth information and acceleration signals at both feature level and decision level for HAR. In their subsequent work [384], the depth image features and acceleration signal features were fed to two computation-efficient collaborative representative classifiers for real-time HAR. Zou et al. [385] proposed two algorithms, namely, EigenGait and TrajGait, to extract acceleration and RGB-D features. Multi-modal

Hybrid Centroid Canonical Correlation Analysis (MHC-CCA) [386] extracted the bag of angles from skeleton data, HP-DMM from depth data, MHI-MEI from RGB data, and statistical features from acceleration data. These features were then fused for multi-modality HAR. Ehatisham et al. [388] proposed a feature-level fusion method based on HOG features extracted from RGB or depth videos, and statistical features extracted from inertial sensors. Malawski and Kwolek [387] proposed an action descriptor, called Joint Motion History Context (JMHC) computed from depth and skeleton data. JMHC, was together with Joint Dynamics (JD) and Local Trace Images (LTI) descriptor on skeleton data, as well as Acc descriptor based on acceleration data, for HAR.

In the work of [324], a DeepConvLSTM model was applied to the combination of acceleration data and gyroscope data. Acceleration data and gyroscope data were also utilized for gait recognition in [391]. Imran and Raman [284] designed a three-stream network architecture, where a 1D-CNN for gyroscopic data, a 2D-CNN for RGB data, and an RNN for skeleton data were used, and late fusion was adopted to predict the final class label. Memmesheimer et al. [389] transformed different modalities as images, and utilized CNN to perform HAR.

Although the aforementioned multi-modality fusion-based HAR methods have achieved promising results on some benchmarks, the task of effective modality fusion is still largely open. Specifically, most of the existing multi-modality methods have complicated model structures that need high computation cost. Thus efficient multi-modality HAR also needs to be addressed.

4.2 CO-LEARNING

Co-learning enabling knowledge transferring between different modalities is also an important problem in HAR, which explores how knowledge learned from one modality can be used to assist the model learning of another modality [354]. Co-learning with multiple modalities often makes up for the shortcomings of a single data modality. It can also benefit the learning when there is a lack of samples for a certain modality, since other correlated modalities with rich samples can be used to assist the model training of this modality in co-learning. Specifically, the data of assistive modalities is only needed during the training process, and is not needed during testing.

4.2.1 Co-Learning with Visual Modalities

Plenty of co-learning-based methods [393], [394], [395] have been introduced for HAR recently, and many of them focused on co-learning with visual modalities, such as RGB with depth modalities and RGB with skeleton modalities, introduced below.

Knowledge transferring [354] between RGB modality capturing appearance information and depth data encoding 3D shape information, has been shown to be able to improve the representation capability of the model of each modality for HAR, especially when one of these modalities has limited annotated data. BHIM [357] and MMHIM [358] are HAR methods that investigated cross-modality learning. Garcia et al. [395] studied multi-stream network learning with modality generalized distillation. Since the latent correlation between modalities is important for cross-modality

recognition, Jia et al. [396] designed a semi-supervised framework utilizing a cross-modality graph coupling RGB and depth modalities to find their correlation and address the problem of missing modalities.

Co-learning between RGB and skeleton modalities has been investigated as well [394]. Thoker and Gall [394] utilized TSN [106] as the teacher network, and ST-GCN [175] and HCN [220] as the student networks, to perform knowledge distillation for cross-modality HAR. Specifically, the teacher network was trained with RGB videos, providing supervision information for the student network handling skeleton data. Song et al. [397] proposed a Modality Compensation Network (MCN) taking advantage of the skeleton modality to compensate the feature learning of the RGB modality with adaptive representation learning, and a modality adaptation block with residual feature learning was designed to bridge information between modalities.

4.2.2 Co-Learning with Visual and Sensor Modalities

There have also been some works [346], [398] for co-learning between visual and sensor modalities, i.e., transferring knowledge amongst these two types of different modalities to enhance the model performance for a certain modality or some modalities. Kong et al. [346] proposed a novel multi-modality distillation model with an attention mechanism, which can transfer adaptive knowledge from sensor modalities to visual ones. Considering the synchronization of vision and sound in videos, Aytar et al. [398] trained deep Sound Networks (SoundNets) by transferring visual knowledge from established vision networks into the sound networks. Alwassel et al. [399] proposed a self-supervised method, called Cross-Modal Deep Clustering (XDC), to utilize the semantic correlation and the differences between RGB and audio modalities. In the work of [400], audio deep learning models were trained, and the visual and acoustic images were exploited in a teacher-student fashion.

5 DATASET

In the past decades, lots of datasets [20], [50], [94], [95], [176], [178], [401] have been proposed for HAR. The significance of the benchmark datasets is self-evident, that facilitates the objective evaluation of HAR methods and promotes the development of the HAR field. In TABLE 5, the information of a series of benchmark datasets with various data modalities is presented. Below we also introduce some of the representative benchmark datasets.

MSR-Action3D [254]. MSR-Action3D dataset, collected by Microsoft and the University of Wollongong in 2010, is the first publicly available dataset providing depth and skeleton modalities for HAR. It contains 20 action classes, and each action was performed by 7 subjects 3 times.

HMDB51 [50]. HMDB51 dataset contains 6,766 manually annotated RGB video clips collected from various sources. It includes 51 action categories, grouped in five types, namely, general facial actions, facial actions with object manipulation, general body movements, body movements with object interaction, and body movements for human interaction.

RGBD-HuDaAct [52]. RGB-HuDaAct dataset, containing RGB and depth modalities, was collected by the Advanced Digital Sciences Center of Singapore, in 2011. It

TABLE 5

Some of the representative benchmark datasets with various data modalities for HAR. Notation: S: Skeleton, D: Depth, IR: Infrared sequence, PC: Point Cloud, ES: Event Stream, Au: Audio, Acc: Acceleration, Gyr: Gyroscope, EMG: electromyography.

Dataset	Reference	Year	Modality	#Class	#Subject	#Sample	#View
KTH	[402]	2004	RGB	6	25	2,391	1
Weizmann	[66]	2005	RGB	10	9	90	1
IXMAS	[70]	2006	RGB	11	10	330	5
HDM05	[403]	2007	RGB,S	130	5	2,337	1
Hollywood	[87]	2008	RGB	8	-	-	430
Hollywood2	[404]	2009	RGB	12	-	3,669	-
MSR-Action3D	[254]	2010	S,D	20	10	567	1
Olympic	[405]	2010	RGB	16	-	783	-
ASLAN	[406]	2011	RGB	432	-	3,697	-
CAD-60	[407]	2011	RGB,S,D	12	4	60	-
HMDB51	[50]	2011	RGB	51	-	6,766	-
RGB-HuDaAct	[52]	2011	RGB,D	13	30	1,189	1
ACT4 ²	[408]	2012	RGB,D	14	24	6,844	4
DHA	[409]	2012	RGB,D	17	21	357	1
MSRDailyActivity3D	[184]	2012	RGB,S,D	16	10	320	1
UCF50	[410]	2012	RGB	50	-	6,681	-
UCF101	[94]	2012	RGB	101	-	13,320	-
UTKinect	[186]	2012	RGB,S,D	10	10	200	1
Berkeley MHAD	[56]	2013	RGB,S,D,Au,Acc	12	12	660	4
CAD-120	[411]	2013	RGB,S,D	10	4	120	-
IAS-lab	[288]	2013	RGB,S,D,PC	15	12	540	1
J-HMDB	[412]	2013	RGB	21	-	31,838	-
MSRAction-Pair	[263]	2013	RGB,S,D	12	10	360	1
UCFKinect	[413]	2013	S	16	16	1,280	1
Multi-View TJU	[414]	2014	RGB,S,D	20	22	7,040	2
Northwestern-UCLA	[415]	2014	RGB,S,D	10	10	1,475	3
Sports-1M	[97]	2014	RGB	487	-	1,113,158	-
UPCV	[416]	2014	S	10	20	400	1
UWA3D Multiview	[289], [417]	2014	RGB,S,D	30	10	1,075	4
ActivityNet	[401]	2015	RGB	203	-	27,801	-
ESC50	[418]	2015	Au	50	-	2,000	-
SYSU 3D HOI	[372]	2015	RGB,S,D	12	40	480	1
TJU	[419]	2015	RGB,S,D	15	20	1,200	1
UTD-MHAD	[347]	2015	RGB,S,D,Acc,Gyr	27	8	861	1
UWA3D Multiview II	[290]	2015	RGB,S,D	30	10	1,075	4
InfAR	[53]	2016	IR	12	40	600	2
NTU RGB+D	[178]	2016	RGB,S,D,IR	60	40	56,880	80
YouTube-8M	[420]	2016	RGB	4,800	-	8,264,650	-
20BN-Something-Something	[421]	2017	RGB	174	-	108,499	-
AVA	[422]	2017	RGB	80	-	437	-
FCVID	[423]	2017	RGB	239	-	91,233	-
Kinetics-400	[95]	2017	RGB	400	-	306,245	-
NEU-UB	[358]	2017	RGB,D	6	20	600	-
PKU-MMD	[51]	2017	RGB,S,D,IR	51	66	21,545	3
UniMiB SHAR	[424]	2017	Acc	17	30	11,771	-
EPIC-KITCHENS	[425]	2018	RGB	-	32	90,000	Egocentric
Kinetics-600	[426]	2018	RGB	600	-	495,547	-
RGB-D Varying-view	[427]	2018	RGB,S,D	40	118	25,600	8+1 covering 360°
DHP19	[55]	2019	ES, S	33	17	-	4
Drive&Act	[428]	2019	RGB,S,D,IR	83	15	-	6
EV-Action	[352]	2019	RGB,S,D,EMG	20	70	7,000	9
HACS	[429]	2019	RGB	200	-	-	-
Kinetics-700	[430]	2019	RGB	700	-	650,317	-
Kitchen20	[431]	2019	Au	20	-	800	-
MMAct	[346]	2019	RGB,S,Acc,Gyr,WiFi,etc.	37	20	36,764	4+Egocentric
Moments in Time	[432]	2019	RGB	339	-	1,000,000	-
NTU RGB+D 120	[176]	2019	RGB,S,D,IR	120	106	114,000	155
ARID	[433]	2020	RGB	11	11	3,784	3

contains 12 categories of daily human activities performed by 30 student volunteers.

CAD-60 [407] and CAD-120 [411]. CAD-60 and CAD-120 datasets were collected by Cornell University. CAD-60 dataset has 60 RGB-D videos of 12 activities, which were performed by 4 subjects in 5 different environments. CAD-120 dataset has 120 RGB-D videos of 10 high-level activities performed by 4 subjects, and each action sample contains RGB frames, depth frames, and skeleton data.

MSRDailyActivity3D [184]. MSRDailyActivity3D dataset was collected by Microsoft and Northwestern University in 2012. This dataset contains 16 activities, performed by 10 people near the sofa. The data modalities of this dataset include RGB, depth, and skeleton.

UCF101 [94]. UCF101 dataset contains 101 action classes

and 13,320 clips. It consists of realistic videos downloaded from YouTube. Various background, lighting, and camera motion conditions make this dataset challenging.

UT-Kinect [186]. UT-Kinect was collected by the University of Texas at Austin in 2012. It contains 10 action classes performed by 10 subjects, and three modalities (RGB, depth, and skeleton joint locations) were synchronously recorded by a single stationary Kinect.

ACT4² [408]. ACT4² dataset is a multi-view RGB-D human action dataset that was collected by the Institute of Computing Technology of Chinese Academy of Science in 2012. It mainly focuses on daily activities. RGB and depth data was captured from 4 different viewpoints using Microsoft Kinect sensors. There are 14 action classes and

6,844 samples.

MSRActionPairs [263]. MSRActionPair dataset was collected by the University of Central Florida and Microsoft in 2013. The actions in this dataset are selected in pairs resulting in similar motions and shapes. RGB, depth, and skeleton data are provided by this dataset.

Berkeley MHAD [56]. The University of California at Berkeley and Johns Hopkins University collected this dataset in 2013. This dataset contains 11 actions performed by 12 people. All the subjects repeated each action 5 times, resulting in about 660 action sequences. Each action was simultaneously captured by five different systems, covering RGB, depth, skeleton, audio, and acceleration data modalities.

UTD-MHAD [347]. UTD-MHAD was collected by the University of Texas at Dallas in 2015. It contains 27 actions performed by 8 subjects, and each action was performed 4 times. RGB videos, depth videos, skeleton joint positions, and the inertial sensor signals (acceleration and gyroscope signals) were recorded.

Kinetics-400 [95]. Kinetics-400, extracted from YouTube, contains 400 human action categories, with 400-1150 clips for each action. The action classes can be grouped into person actions (singular), person-person actions, and person-object actions. This dataset has been further extended to Kinetics-600 [426] and Kinetics-700 [430].

PKU-MMD [51]. PKU-MMD covers 51 action categories with 1,076 long video sequences for continuous multi-modality 3D action analysis. It was collected with the Kinect v2 sensors providing multi-modality data, including RGB, depth, skeleton, and infrared radiation.

MMAct [346]. Multi-Modal Action dataset (MMAct) is a large-scale dataset for multi-modality human action analysis, which covers seven modalities, namely, RGB videos, skeleton, acceleration, gyroscope, orientation, WiFi, and pressure signals.

NTU RGB+D [178] and NTU RGB+D 120 [176]. NTU RGB+D and NTU RGB+D 120 datasets were collected with Microsoft Kinect v2 sensors providing depth maps, 3D joint information, RGB frames, and infrared sequences. There are 60 action classes, 40 distinct subjects, 56,880 samples from 80 views in the NTU RGB+D dataset, while its extended version, NTU RGB+D 120 dataset, is a very large multi-modality HAR dataset containing 120 action categories and 114,480 samples.

6 DISCUSSION

In the previous sections, we review the methods and datasets for HAR with various data modalities. Below we discuss some of the potential and important directions that could need further investigation in this domain.

Dataset. Large and comprehensive datasets generally have vital importance for the development of HAR, especially for the deep learning-based HAR methods. There are many aspects to indicate the quality of a dataset, such as the size, diversities, applicability, labels, and modalities, etc. Despite the large number of existing datasets that have prompted the HAR area greatly, to further facilitate the research on HAR, new benchmark datasets with higher

qualities in multiple aspects still need to be further developed. For example, most of the existing multi-modality datasets were collected in controlled environments, where actions were usually performed by volunteers. Thus collecting multi-modality data from uncontrolled environments to achieve large and challenging benchmarks for further promoting multi-modality HAR application in practical scenarios, can be important. Besides, the construction of large and challenging datasets for group action recognition can be further investigated as well.

Multi-modality Learning. As discussed in Section 4, plenty of multi-modality learning methods, including multi-modality fusion and cross-modality transfer learning, have been designed for HAR, since the fusion of multi-modality data can often complement each other to improve the HAR performance, while co-learning can be used to alleviate the issue of data lack for some modalities. However, as pointed out by [434], many existing multi-modality methods are not effective as expected owing to a series of challenges, such as over-fitting. This implies that there remains a large space for designing more effective fusion and co-learning strategies for multi-modality HAR.

Efficient Action Analysis. The superior performance of many HAR methods is built on high computational complexity, while efficient HAR is also crucial for many practical applications. Hence how to reduce the computational cost and resource consumption (e.g., CPU, GPU, and energy consumption, etc.), and achieve efficient and fast HAR, is worth further study as well.

Early Action Recognition. Early action recognition (action prediction) enables recognition when only a part of the action has been performed, i.e., recognizing an action before it is fully performed [392], [435], [436]. This is also an important problem due to its relevance to some applications, such as online human-robot interaction and early alarm in some scenarios.

Few-shot Action Analysis. It can be difficult to collect a large amount of training data (especially the multi-modality data) for all action classes. To handle this issue, one of the possible solutions is taking advantage of few-shot learning techniques [437]. Though there have been some attempts for few-shot HAR [176], [438], considering the significance of handling the data lack issue in many practical scenarios, more advanced few-shot action analysis can still be further studied.

Unsupervised and Semi-supervised Learning. Supervised learning methods, especially deep learning-based supervised learning methods, often require a large amount of data with expensive labels for model training. Meanwhile, unsupervised and semi-supervised learning techniques [361], [396] often enable us to leverage unlabelled data to train the models, which significantly reduces the requirement of labeled data. Since unlabelled action samples are often easier to be collected than labeled sequences, unsupervised and semi-supervised HAR also becomes an important direction that is worth of further development.

7 CONCLUSION

HAR is an important task that has attracted contiguous research attention in the past decades, and various data

modalities with different characteristics have been applied for this task. In this paper, we have given a comprehensive review of HAR methods using different data modalities, including RGB, skeleton, depth, infrared sequence, point cloud, event stream, audio, acceleration, radar, and WiFi, etc. Multi-modality recognition methods, including multi-modality fusion and cross-modality co-learning methods, have been surveyed as well. The benchmark datasets have also been reviewed. Besides, we have discussed some potential research directions in this paper.

REFERENCES

- [1] S. Danafar and N. Gheissari, "Action recognition for surveillance applications using optic flow and svm," in *ACCV*.
- [2] L. Chen, N. Ma, P. Wang, J. Li, P. Wang, G. Pang, and X. Shi, "Survey of pedestrian action recognition techniques for autonomous driving," *Tsinghua Science and Technology*, vol. 25, no. 4.
- [3] W. Hu, D. Xie, Z. Fu, W. Zeng, and S. Maybank, "Semantic-based surveillance video retrieval," *TIP*, vol. 16, no. 4.
- [4] I. Rodomagoulakis, N. Kardaris, V. Pitsikalis, E. Mavroudi, A. Katsamanis, A. Tsiami, and P. Maragos, "Multimodal human action recognition in assistive human-robot interaction," in *ICASSP*.
- [5] R. Poppe, "A survey on vision-based human action recognition," *Image and vision computing*, vol. 28, no. 6.
- [6] J. Donahue, L. Anne Hendricks, S. Guadarrama, M. Rohrbach, S. Venugopalan, K. Saenko, and T. Darrell, "Long-term recurrent convolutional networks for visual recognition and description," in *CVPR*.
- [7] J. Liu, A. Shahroudy, D. Xu, A. C. Kot, and G. Wang, "Skeleton-based action recognition using spatio-temporal lstm network with trust gates," *TPAMI*, vol. 40, no. 12.
- [8] H. Rahmani and A. Mian, "3d action recognition from novel viewpoints," in *CVPR*.
- [9] Z. Jiang, V. Rozgic, and S. Adali, "Learning spatiotemporal features for infrared action recognition with 3d convolutional neural networks," in *CVPRW*.
- [10] Y. Wang, Y. Xiao, F. Xiong, W. Jiang, Z. Cao, J. T. Zhou, and J. Yuan, "3dv: 3d dynamic voxel for action recognition in depth video," in *CVPRn*.
- [11] Y. Bi and Y. Andreopoulos, "Pix2nvs: Parameterized conversion of pixel-domain video frames to neuromorphic vision streams," in *ICIP*.
- [12] R. Gao, T.-H. Oh, K. Grauman, and L. Torresani, "Listen to look: Action recognition by previewing audio," in *CVPR*.
- [13] M. Zeng, L. T. Nguyen, B. Yu, O. J. Mengshoel, J. Zhu, P. Wu, and J. Zhang, "Convolutional neural networks for human activity recognition using mobile sensors," in *MobiCASE*, 2014.
- [14] Y. Kim and T. Moon, "Human detection and activity classification based on micro-doppler signatures using deep convolutional neural networks," *GRLS*, vol. 13, no. 1.
- [15] Y. Wang, J. Liu, Y. Chen, M. Gruteser, J. Yang, and H. Liu, "E-eyes: device-free location-oriented activity identification using fine-grained wifi signatures," in *MobiCom*.
- [16] N. A. Maffioletti, M. Gorelick, I. Kramers-de Quervain, M. Bizzini, J. P. Munzinger, S. Tomasetti, and A. Stacoff, "Concurrent validity and intrasession reliability of the idea accelerometry system for the quantification of spatiotemporal gait parameters," *Gait & posture*, vol. 27, no. 1.
- [17] E. Kazakos, A. Nagrani, A. Zisserman, and D. Damen, "Epic-fusion: Audio-visual temporal binding for egocentric action recognition,"
- [18] P. Wang, W. Li, J. Wan, P. Ogunbona, and X. Liu, "Cooperative training of deep aggregation networks for rgb-d action recognition," in *AAAI*, 2018.
- [19] R. Lun and W. Zhao, "A survey of applications and human motion recognition with microsoft kinect," *Int. J. Pattern Recognit. Artif. Intell.*, vol. 29, no. 05.
- [20] J. Zhang, W. Li, P. O. Ogunbona, P. Wang, and C. Tang, "Rgb-d-based action recognition datasets: A survey," *Pattern Recognition*, vol. 60.
- [21] F. Zhu, L. Shao, J. Xie, and Y. Fang, "From handcrafted to learned representations for human action recognition: a survey," *Image and Vision Computing*, vol. 55.
- [22] S. Herath, M. Harandi, and F. Porikli, "Going deeper into action recognition: A survey," *Image and vision computing*, vol. 60.
- [23] M. Koohzadi and N. M. Charkari, "Survey on deep learning methods in human action recognition," *IET Computer Vision*, vol. 11, no. 8.
- [24] Y. Kong and Y. Fu, "Human action recognition and prediction: A survey," *arXiv preprint arXiv:1806.11230*, 2018.
- [25] P. Wang, W. Li, P. Ogunbona, J. Wan, and S. Escalera, "Rgb-d-based human motion recognition with deep learning: A survey," *CVIU*, vol. 171.
- [26] H.-B. Zhang, Y.-X. Zhang, B. Zhong, Q. Lei, L. Yang, J.-X. Du, and D.-S. Chen, "A comprehensive survey of vision-based human action recognition methods," *Sensors*, vol. 19, no. 5.
- [27] L. Wang, D. Q. Huynh, and P. Koniusz, "A comparative review of recent kinect-based action recognition algorithms," *TIP*, vol. 29.
- [28] Z. Zhang, "Microsoft kinect sensor and its effect," *IEEE multimedia*, vol. 19, no. 2.
- [29] I. Jegham, A. B. Khalifa, I. Alouani, and M. A. Mahjoub, "Vision-based human action recognition: An overview and real world challenges," *Forensic Science International: Digital Investigation*, vol. 32.
- [30] P. Turaga, R. Chellappa, V. S. Subrahmanian, and O. Udrea, "Machine recognition of human activities: A survey," *TCSVT*, vol. 18, no. 11.
- [31] D. Weinland, R. Ronfard, and E. Boyer, "A survey of vision-based methods for action representation, segmentation and recognition," *CVIU*, vol. 115, no. 2.
- [32] J. K. Aggarwal and M. S. Ryoo, "Human activity analysis: A review," *ACM Computing Surveys*, vol. 43, no. 3.
- [33] J. M. Chaquet, E. J. Carmona, and A. Fernández-Caballero, "A survey of video datasets for human action and activity recognition," *CVIU*, vol. 117, no. 6.
- [34] G. Guo and A. Lai, "A survey on still image based human action recognition," *Pattern Recognition*, vol. 47, no. 10.
- [35] J. K. Aggarwal and L. Xia, "Human activity recognition from 3d data: A review," *Pattern Recognit. Lett.*, vol. 48.
- [36] L. L. Presti and M. La Cascia, "3d skeleton-based human action classification: A survey," *Pattern Recognition*, vol. 53.
- [37] F. Han, B. Reily, W. Hoff, and H. Zhang, "Space-time representation of people based on 3d skeletal data: A review," *CVIU*, vol. 158.
- [38] B. Ren, M. Liu, R. Ding, and H. Liu, "A survey on 3d skeleton-based action recognition using learning method," *arXiv preprint arXiv:2002.05907*, 2020.
- [39] L. Chen, H. Wei, and J. Ferryman, "A survey of human motion analysis using depth imagery," *Pattern Recognit. Lett.*, vol. 34, no. 15.
- [40] M. Ye, Q. Zhang, L. Wang, J. Zhu, R. Yang, and J. Gall, "A survey on human motion analysis from depth data," in *Time-of-flight and depth imaging. sensors, algorithms, and applications*.
- [41] C. Chen, R. Jafari, and N. Kehtarnavaz, "A survey of depth and inertial sensor fusion for human action recognition," *Multimed. Tools. Appl.*, vol. 76, no. 3.
- [42] A. Avci, S. Bosch, M. Marin-Perianu, R. Marin-Perianu, and P. Havinga, "Activity recognition using inertial sensing for healthcare, wellbeing and sports applications: A survey," in *ARCS*.
- [43] L. Chen, J. Hoey, C. D. Nugent, D. J. Cook, and Z. Yu, "Sensor-based activity recognition," *SMC*, vol. 42, no. 6.
- [44] O. D. Lara and M. A. Labrador, "A survey on human activity recognition using wearable sensors," *IEEE Communications Surveys & Tutorials*, vol. 3, no. 15.
- [45] M. Shoaib, S. Bosch, O. D. Incel, H. Scholten, and P. J. Havinga, "A survey of online activity recognition using mobile phones," *Sensors*, vol. 15, no. 1.
- [46] S. Yousefi, H. Narui, S. Dayal, S. Ermon, and S. Valaee, "A survey on behavior recognition using wifi channel state information," *IEEE Commun. Mag.*, vol. 55, no. 10, 2017.
- [47] J. Wang, Y. Chen, S. Hao, X. Peng, and L. Hu, "Deep learning for sensor-based activity recognition: A survey," *Pattern Recognition Letters*, vol. 119.
- [48] S. Slim, A. Atia, M. Elfattah, and M. Mostafa, "Survey on human activity recognition based on acceleration data," *Intl. J. Adv. Comput. Sci. Appl.*, vol. 10.
- [49] X. Li, Y. He, and X. Jing, "A survey of deep learning-based human activity recognition in radar," *Remote Sensing*, vol. 11, no. 9.

- [50] H. Kuehne, H. Jhuang, E. Garrote, T. Poggio, and T. Serre, "Hmdb: a large video database for human motion recognition," in *ICCV*.
- [51] C. Liu, Y. Hu, Y. Li, S. Song, and J. Liu, "Pku-mmd: A large scale benchmark for continuous multi-modal human action understanding," *arXiv preprint arXiv:1703.07475*, 2017.
- [52] B. Ni, G. Wang, and P. Moulin, "Rgb-d-hudaact: A color-depth video database for human daily activity recognition," in *ICCVW*.
- [53] C. Gao, Y. Du, J. Liu, J. Lv, L. Yang, D. Meng, and A. G. Hauptmann, "Infar dataset: Infrared action recognition at different times," *Neurocomputing*, vol. 212.
- [54] H. Cheng and S. M. Chung, "Orthogonal moment-based descriptors for pose shape query on 3d point cloud patches," *Pattern Recognition*, vol. 52.
- [55] E. Calabrese, G. Taverni, C. Awai Easthope, S. Skriabine, F. Corradi, L. Longinotti, K. Eng, and T. Delbruck, "Dhp19: Dynamic vision sensor 3d human pose dataset," in *CVPRW*.
- [56] F. Offi, R. Chaudhry, G. Kurillo, R. Vidal, and R. Bajcsy, "Berkeley mhad: A comprehensive multimodal human action database," in *WACV*.
- [57] J. R. Kwapisz, G. M. Weiss, and S. A. Moore, "Activity recognition using cell phone accelerometers," *ACM SigKDD Explorations Newsletter*, vol. 12, no. 2.
- [58] W. Wang, A. X. Liu, M. Shahzad, K. Ling, and S. Lu, "Understanding and modeling of wifi signal based human activity recognition," in *MobiCom*.
- [59] T. Young, "Li. the bakerian lecture. on the theory of light and colours," *Philosophical transactions of the Royal Society of London*, no. 92.
- [60] W. Lin, M.-T. Sun, R. Poovandran, and Z. Zhang, "Human activity recognition for video surveillance," in *ISCAS*.
- [61] M. Lu, Y. Hu, and X. Lu, "Driver action recognition using deformable and dilated faster r-cnn with optimized region proposals," *Applied Intelligence*, vol. 50, no. 4.
- [62] K. Soomro and A. R. Zamir, "Action recognition in realistic sports videos," in *Computer vision in sports*.
- [63] B. Yao and L. Fei-Fei, "Grouplet: A structured image representation for recognizing human and object interactions," in *CVPR*.
- [64] G. Sharma, F. Jurie, and C. Schmid, "Discriminative spatial saliency for image classification," in *CVPR*.
- [65] B. Yao and L. Fei-Fei, "Modeling mutual context of object and human pose in human-object interaction activities," in *CVPR*.
- [66] L. Gorelick, M. Blank, E. Shechtman, M. Irani, and R. Basri, "Actions as space-time shapes," *TPAMI*, vol. 29, no. 12.
- [67] I. Laptev, "On space-time interest points," *IJCV*, vol. 64, no. 2-3.
- [68] H. Wang and C. Schmid, "Action recognition with improved trajectories," in *ICCV*.
- [69] A. F. Bobick and J. W. Davis, "The recognition of human movement using temporal templates," *TPAMI*, vol. 23, no. 3.
- [70] D. Weinland, R. Ronfard, and E. Boyer, "Free viewpoint action recognition using motion history volumes," *CVIU*, vol. 104, no. 2-3.
- [71] A. Yilmaz and M. Shah, "Actions sketch: A novel action representation," in *CVPR*, vol. 1.
- [72] S. Ali and M. Shah, "Human action recognition in videos using kinematic features and multiple instance learning," *TPAMI*, vol. 32, no. 2.
- [73] A. A. Efros, A. C. Berg, G. Mori, and J. Malik, "Recognizing action at a distance," in *ICCV*.
- [74] D. D. Dawn and S. H. Shaikh, "A comprehensive survey of human action recognition with spatio-temporal interest point (stip) detector," *The Vis. Comp.*, vol. 32, no. 3.
- [75] G. Willems, T. Tuytelaars, and L. Van Gool, "An efficient dense and scale-invariant spatio-temporal interest point detector," in *ECCV*.
- [76] P. Dollár, V. Rabaud, G. Cottrell, and S. Belongie, "Behavior recognition via sparse spatio-temporal features," in *VS-PETS*.
- [77] P. Scovanner, S. Ali, and M. Shah, "A 3-dimensional sift descriptor and its application to action recognition," in *ACM Multimedia*.
- [78] A. Klaser, M. Marszałek, and C. Schmid, "A spatio-temporal descriptor based on 3d-gradients," 2008.
- [79] L. Yefet and L. Wolf, "Local trinary patterns for human action recognition," in *ICCV*.
- [80] J. C. Niebles, H. Wang, and L. Fei-Fei, "Unsupervised learning of human action categories using spatial-temporal words," *IJCV*, vol. 79, no. 3.
- [81] X. Peng, L. Wang, X. Wang, and Y. Qiao, "Bag of visual words and fusion methods for action recognition: Comprehensive study and good practice," *CVIU*, vol. 150.
- [82] C. G. Harris, M. Stephens, *et al.*, "A combined corner and edge detector," in *Alvey vision conference*, vol. 15.
- [83] S.-F. Wong and R. Cipolla, "Extracting spatiotemporal interest points using global information," in *ICCV*.
- [84] H. Wang, M. M. Ullah, A. Klaser, I. Laptev, and C. Schmid, "Evaluation of local spatio-temporal features for action recognition," in *BMVC*, 2009.
- [85] J. Liu, J. Luo, and M. Shah, "Recognizing realistic actions from videos "in the wild"," in *CVPR*.
- [86] H. Wang, A. Kläser, C. Schmid, and C.-L. Liu, "Dense trajectories and motion boundary descriptors for action recognition," *IJCV*, vol. 103, no. 1.
- [87] I. Laptev, M. Marszałek, C. Schmid, and B. Rozenfeld, "Learning realistic human actions from movies," in *CVPR*.
- [88] N. Dalal and B. Triggs, "Histograms of oriented gradients for human detection," in *CVPR*, vol. 1.
- [89] N. Dalal, B. Triggs, and C. Schmid, "Human detection using oriented histograms of flow and appearance," in *ECCV*.
- [90] H. Bay, T. Tuytelaars, and L. Van Gool, "Surf: Speeded up robust features," in *ECCV*.
- [91] A. Gaidon, Z. Harchaoui, and C. Schmid, "Activity representation with motion hierarchies," *IJCV*, vol. 107, no. 3.
- [92] X. Peng, C. Zou, Y. Qiao, and Q. Peng, "Action recognition with stacked fisher vectors," in *ECCV*.
- [93] H. Wang, D. Oneata, J. Verbeek, and C. Schmid, "A robust and efficient video representation for action recognition," *IJCVn*, vol. 119, no. 3.
- [94] K. Soomro, A. R. Zamir, and M. Shah, "Ucf101: A dataset of 101 human actions classes from videos in the wild," *arXiv preprint arXiv:1212.0402*, 2012.
- [95] W. Kay, J. Carreira, K. Simonyan, B. Zhang, C. Hillier, S. Vijayanarasimhan, F. Viola, T. Green, T. Back, P. Natsev, *et al.*, "The kinetics human action video dataset," *arXiv preprint arXiv:1705.06950*, 2017.
- [96] D. Tran, L. Bourdev, R. Fergus, L. Torresani, and M. Paluri, "Learning spatiotemporal features with 3d convolutional networks," in *ICCV*.
- [97] A. Karpathy, G. Toderici, S. Shetty, T. Leung, R. Sukthankar, and L. Fei-Fei, "Large-scale video classification with convolutional neural networks," in *CVPR*.
- [98] K. Simonyan and A. Zisserman, "Two-stream convolutional networks for action recognition in videos," in *NeurIPS*.
- [99] G. Chéron, I. Laptev, and C. Schmid, "P-cnn: Pose-based cnn features for action recognition," in *ICCV*.
- [100] L. Wang, Y. Xiong, Z. Wang, and Y. Qiao, "Towards good practices for very deep two-stream convnets," *arXiv preprint arXiv:1507.02159*, 2015.
- [101] L. Wang, Y. Qiao, and X. Tang, "Action recognition with trajectory-pooled deep-convolutional descriptors," in *CVPR*.
- [102] B. Zhang, L. Wang, Z. Wang, Y. Qiao, and H. Wang, "Real-time action recognition with enhanced motion vector cnns," in *CVPR*.
- [103] X. Wang, A. Farhadi, and A. Gupta, "Actions" transformations," in *CVPR*.
- [104] Y. Wang, J. Song, L. Wang, L. Van Gool, and O. Hilliges, "Two-stream sr-cnns for action recognition in videos.," in *BMVC*, 2016.
- [105] C. Feichtenhofer, A. Pinz, and A. Zisserman, "Convolutional two-stream network fusion for video action recognition," in *CVPR*.
- [106] L. Wang, Y. Xiong, Z. Wang, Y. Qiao, D. Lin, X. Tang, and L. Van Gool, "Temporal segment networks: Towards good practices for deep action recognition," in *ECCV*.
- [107] C. Feichtenhofer, A. Pinz, and R. P. Wildes, "Spatiotemporal residual networks for video action recognition. corr abs/1611.02155 (2016)," *arXiv preprint arXiv:1611.02155*, 2016.
- [108] R. Girdhar and D. Ramanan, "Attentional pooling for action recognition," in *NeurIPS*.
- [109] X. Wang, L. Gao, P. Wang, X. Sun, and X. Liu, "Two-stream 3-d convnet fusion for action recognition in videos with arbitrary size and length," *TMM*, vol. 20, no. 3.
- [110] A. Kar, N. Rai, K. Sikka, and G. Sharma, "Adascan: Adaptive scan pooling in deep convolutional neural networks for human action recognition in videos," in *CVPR*.
- [111] R. Girdhar, D. Ramanan, A. Gupta, J. Sivic, and B. Russell, "Actionvlad: Learning spatio-temporal aggregation for action classification," in *CVPR*.

- [112] I. C. Duta, B. Ionescu, K. Aizawa, and N. Sebe, "Spatio-temporal vector of locally max pooled features for action recognition in videos," in *CVPR*.
- [113] C. Feichtenhofer, A. Pinz, and R. P. Wildes, "Spatiotemporal multiplier networks for video action recognition," in *CVPR*.
- [114] Z. Lan, Y. Zhu, A. G. Hauptmann, and S. Newsam, "Deep local video feature for action recognition," in *CVPRW*.
- [115] A. Diba, V. Sharma, and L. Van Gool, "Deep temporal linear encoding networks," in *CVPR*.
- [116] Y. Zhu, Z. Lan, S. Newsam, and A. Hauptmann, "Hidden two-stream convolutional networks for action recognition," in *ACCV*.
- [117] C. Feichtenhofer, H. Fan, J. Malik, and K. He, "Slowfast networks for video recognition," in *ICCV*.
- [118] H. Zhang, D. Liu, and Z. Xiong, "Two-stream action recognition-oriented video super-resolution," in *ICCV*.
- [119] M. Tong, M. Zhao, Y. Chen, and H. Wang, "D3-Ind: A two-stream framework with discriminant deep descriptor, linear cmdt and nonlinear kcmdt descriptors for action recognition," *Neurocomputing*, vol. 325.
- [120] E. Chen, X. Bai, L. Gao, H. C. Tinega, and Y. Ding, "A spatiotemporal heterogeneous two-stream network for action recognition," *IEEE Access*, vol. 7.
- [121] Y. Wan, Z. Yu, Y. Wang, and X. Li, "Action recognition based on two-stream convolutional networks with long-short-term spatiotemporal features," *IEEE Access*, vol. 8.
- [122] M. Baccouche, F. Mamalet, C. Wolf, C. Garcia, and A. Baskurt, "Sequential deep learning for human action recognition," in *HBUI*.
- [123] S. Sharma, R. Kiros, and R. Salakhutdinov, "Action recognition using visual attention," *arXiv preprint arXiv:1511.04119*, 2015.
- [124] N. Srivastava, E. Mansimov, and R. Salakhutdinov, "Unsupervised learning of video representations using lstms," in *ICML*.
- [125] J. Yue-Hei Ng, M. Hausknecht, S. Vijayanarasimhan, O. Vinyals, R. Monga, and G. Toderici, "Beyond short snippets: Deep networks for video classification," in *CVPR*.
- [126] Z. Wu, X. Wang, Y.-G. Jiang, H. Ye, and X. Xue, "Modeling spatial-temporal clues in a hybrid deep learning framework for video classification," in *ACM Multimedia*.
- [127] X. Wang, L. Gao, J. Song, and H. Shen, "Beyond frame-level cnn: saliency-aware 3-d cnn with lstm for video action recognition," *IEEE Signal Processing Letters*, vol. 24, no. 4.
- [128] A. Ullah, J. Ahmad, K. Muhammad, M. Sajjad, and S. W. Baik, "Action recognition in video sequences using deep bi-directional lstm with cnn features," *IEEE Access*, vol. 6.
- [129] L. Sun, K. Jia, K. Chen, D.-Y. Yeung, B. E. Shi, and S. Savarese, "Lattice long short-term memory for human action recognition," in *ICCV*.
- [130] H. Ge, Z. Yan, W. Yu, and L. Sun, "An attention mechanism based convolutional lstm network for video action recognition," *Multimed. Tools. Appl.*, vol. 78, no. 14.
- [131] X. Ouyang, S. Xu, C. Zhang, P. Zhou, Y. Yang, G. Liu, and X. Li, "A 3d-cnn and lstm based multi-task learning architecture for action recognition," *IEEE Access*, vol. 7.
- [132] Y. Pan, J. Xu, M. Wang, J. Ye, F. Wang, K. Bai, and Z. Xu, "Compressing recurrent neural networks with tensor ring for action recognition," in *AAAI*, vol. 33.
- [133] Z. Liu, Z. Li, R. Wang, M. Zong, and W. Ji, "Spatiotemporal saliency-based multi-stream networks with attention-aware lstm for action recognition," *Neural. Comput. Appl.s*.
- [134] M. Majd and R. Safabakhsh, "Correlational convolutional lstm for human action recognition," *Neurocomputing*, vol. 396.
- [135] A. Mihanpour, M. J. Rashti, and S. E. Alavi, "Human action recognition in video using db-lstm and resnet," in *ICWR*.
- [136] S. Ji, W. Xu, M. Yang, and K. Yu, "3d convolutional neural networks for human action recognition," *TPAMI*, vol. 35, no. 1.
- [137] L. Sun, K. Jia, D.-Y. Yeung, and B. E. Shi, "Human action recognition using factorized spatio-temporal convolutional networks," in *ICCV*.
- [138] G. Varol, I. Laptev, and C. Schmid, "Long-term temporal convolutions for action recognition," *TPAMI*, vol. 40, no. 6.
- [139] A. Diba, M. Fayyaz, V. Sharma, A. H. Karami, M. M. Arzani, R. Yousefzadeh, and L. Van Gool, "Temporal 3d convnets: New architecture and transfer learning for video classification," *arXiv preprint arXiv:1711.08200*, 2017.
- [140] J. Carreira and A. Zisserman, "Quo vadis, action recognition? a new model and the kinetics dataset," in *CVPR*.
- [141] Z. Qiu, T. Yao, and T. Mei, "Learning spatio-temporal representation with pseudo-3d residual networks," in *ICCV*.
- [142] L. Wang, W. Li, W. Li, and L. Van Gool, "Appearance-and-relation networks for video classification," in *CVPR*.
- [143] Y. Zhou, X. Sun, Z.-J. Zha, and W. Zeng, "Mict: Mixed 3d/2d convolutional tube for human action recognition," in *CVPR*.
- [144] M. Zolfaghari, K. Singh, and T. Brox, "Eco: Efficient convolutional network for online video understanding," in *ECCV*.
- [145] A. Diba, M. Fayyaz, V. Sharma, M. Mahdi Arzani, R. Yousefzadeh, J. Gall, and L. Van Gool, "Spatio-temporal channel correlation networks for action classification," in *ECCV*.
- [146] D. Tran, H. Wang, L. Torresani, J. Ray, Y. LeCun, and M. Paluri, "A closer look at spatiotemporal convolutions for action recognition," in *CVPR*.
- [147] H. Yang, C. Yuan, B. Li, Y. Du, J. Xing, W. Hu, and S. J. Maybank, "Asymmetric 3d convolutional neural networks for action recognition," *Pattern recognition*, vol. 85.
- [148] Y. Huang, Y. Guo, and C. Gao, "Efficient parallel inflated 3d convolution architecture for action recognition," *IEEE Access*, vol. 8.
- [149] J. Li, X. Liu, M. Zhang, and D. Wang, "Spatio-temporal deformable 3d convnets with attention for action recognition," *Pattern Recognition*, vol. 98.
- [150] J. Stroud, D. Ross, C. Sun, J. Deng, and R. Sukthankar, "D3d: Distilled 3d networks for video action recognition," in *WACV*.
- [151] B. Zhou, A. Andonian, A. Oliva, and A. Torralba, "Temporal relational reasoning in videos," in *ECCV*.
- [152] H. Gammulle, S. Denman, S. Sridharan, and C. Fookes, "Two stream lstm: A deep fusion framework for human action recognition," in *WACV*.
- [153] C. Dai, X. Liu, and J. Lai, "Human action recognition using two-stream attention based lstm networks," *Applied soft computing*, vol. 86.
- [154] J. Gao, T. Zhang, and C. Xu, "I know the relationships: Zero-shot action recognition via two-stream graph convolutional networks and knowledge graphs," in *AAAI*, vol. 33.
- [155] R. Arandjelovic, P. Gronat, A. Torii, T. Pajdla, and J. Sivic, "Netvlad: Cnn architecture for weakly supervised place recognition," in *CVPR*.
- [156] W. Du, Y. Wang, and Y. Qiao, "Rpan: An end-to-end recurrent pose-attention network for action recognition in videos," in *ICCV*.
- [157] T. Perrett and D. Damen, "Ddlstm: Dual-domain lstm for cross-dataset action recognition," in *CVPR*.
- [158] M. C. Leong, D. K. Prasad, Y. T. Lee, and F. Lin, "Semi-cnn architecture for effective spatio-temporal learning in action recognition," *Applied Sciences*, vol. 10, no. 2.
- [159] G. Huang, Z. Liu, L. Van Der Maaten, and K. Q. Weinberger, "Densely connected convolutional networks," in *CVPR*.
- [160] N. Hussein, E. Gavves, and A. W. Smeulders, "Timeception for complex action recognition," in *CVPR*.
- [161] H. Ling, Y. Chen, J. Chen, L. Wu, Y. Shi, and J. Deng, "Xwisenet: action recognition with xwise separable convolutions," *Multimed. Tools. Appl.*
- [162] G. Varol, I. Laptev, and C. Schmid, "Long-term temporal convolutions for action recognition," *TPAMI*, vol. 40, no. 6.
- [163] R. Girdhar, J. Carreira, C. Doersch, and A. Zisserman, "Video action transformer network," in *CVPR*.
- [164] G. W. Taylor, R. Fergus, Y. LeCun, and C. Bregler, "Convolutional learning of spatio-temporal features," in *ECCV*.
- [165] K. Sun, B. Xiao, D. Liu, and J. Wang, "Deep high-resolution representation learning for human pose estimation," in *CVPR*.
- [166] I. Akhter and M. J. Black, "Pose-conditioned joint angle limits for 3d human pose reconstruction," in *CVPR*.
- [167] D. Mehta, S. Sridhar, O. Sotnychenko, H. Rhodin, M. Shafiei, H.-P. Seidel, W. Xu, D. Casas, and C. Theobalt, "Vnect: Real-time 3d human pose estimation with a single rgb camera," *TOG*, vol. 36, no. 4.
- [168] S. Yang, J. Liu, S. Lu, M. H. Er, and A. C. Kot, "Collaborative learning of gesture recognition and 3d hand pose estimation with multi-order feature analysis," in *ECCV*.
- [169] J. Shotton, A. Fitzgibbon, M. Cook, T. Sharp, M. Finocchio, R. Moore, A. Kipman, and A. Blake, "Real-time human pose recognition in parts from single depth images," in *CVPR*.
- [170] R. Girshick, J. Shotton, P. Kohli, A. Criminisi, and A. Fitzgibbon, "Efficient regression of general-activity human poses from depth images," in *ICCV*.

- [171] M. Ye, X. Wang, R. Yang, L. Ren, and M. Pollefeys, "Accurate 3d pose estimation from a single depth image," in *ICCV*.
- [172] C. Plagemann, V. Ganapathi, D. Koller, and S. Thrun, "Real-time identification and localization of body parts from depth images," in *ICRA*.
- [173] J. Taylor, J. Shotton, T. Sharp, and A. Fitzgibbon, "The vitruvian manifold: Inferring dense correspondences for one-shot human pose estimation," in *CVPR*.
- [174] A. Baak, M. Müller, G. Bharaj, H.-P. Seidel, and C. Theobalt, "A data-driven approach for real-time full body pose reconstruction from a depth camera," in *Consumer Depth Cameras for Computer Vision*.
- [175] S. Yan, Y. Xiong, and D. Lin, "Spatial temporal graph convolutional networks for skeleton-based action recognition," in *AAAI*, 2018.
- [176] J. Liu, A. Shahroudy, M. L. Perez, G. Wang, L.-Y. Duan, and A. C. Kot, "Ntu rgb+d 120: A large-scale benchmark for 3d human activity understanding," *TPAMI*, 2020.
- [177] Q. Ke, J. Liu, M. Bennamoun, H. Rahmani, S. An, F. Sohel, and F. Boussaid, "Global regularizer and temporal-aware cross-entropy for skeleton-based early action recognition," in *ACCV*.
- [178] A. Shahroudy, J. Liu, T.-T. Ng, and G. Wang, "Ntu rgb+d: A large scale dataset for 3d human activity analysis," in *CVPR*.
- [179] Y. Zhu, W. Chen, and G. Guo, "Fusing spatiotemporal features and joints for 3d action recognition," in *CVPRW*.
- [180] B. Xiaohan Nie, C. Xiong, and S.-C. Zhu, "Joint action recognition and pose estimation from video," in *CVPR*.
- [181] A. A. Chaaoui, J. R. Padilla-López, P. Climent-Pérez, and F. Flórez-Revueña, "Evolutionary joint selection to improve human action recognition with rgb-d devices," *Expert Syst. Appl.*, vol. 41, no. 3.
- [182] R. Vemulapalli, F. Arrate, and R. Chellappa, "Human action recognition by representing 3d skeletons as points in a lie group," in *CVPR*.
- [183] F. Ofli, R. Chaudhry, G. Kurillo, R. Vidal, and R. Bajcsy, "Sequence of the most informative joints (smij): A new representation for human skeletal action recognition," *J. Vis. Commun. Image Represent.*, vol. 25, no. 1.
- [184] J. Wang, Z. Liu, Y. Wu, and J. Yuan, "Mining actionlet ensemble for action recognition with depth cameras," in *CVPR*.
- [185] J. Wang, Z. Liu, Y. Wu, and J. Yuan, "Learning actionlet ensemble for 3d human action recognition," *TPAMI*, vol. 36, no. 5.
- [186] L. Xia, C.-C. Chen, and J. K. Aggarwal, "View invariant human action recognition using histograms of 3d joints," in *CVPRW*.
- [187] X. Yang and Y. L. Tian, "Eigenjoints-based action recognition using naive-bayes-nearest-neighbor," in *CVPRW*.
- [188] X. Yang and Y. Tian, "Effective 3d action recognition using eigenjoints," *Vis. Commun. and Image Represent.*, vol. 25, no. 1.
- [189] M. E. Hussein, M. Torki, M. A. Gowayyed, and M. El-Saban, "Human action recognition using a temporal hierarchy of covariance descriptors on 3d joint locations," in *IJCAI*, 2013.
- [190] M. A. Gowayyed, M. Torki, M. E. Hussein, and M. El-Saban, "Histogram of oriented displacements (hod): Describing trajectories of human joints for action recognition," in *IJCAI*, 2013.
- [191] G. Evangelidis, G. Singh, and R. Horaud, "Skeletal quads: Human action recognition using joint quadruples," in *ICPR*.
- [192] R. Chaudhry, F. Ofli, G. Kurillo, R. Bajcsy, and R. Vidal, "Bio-inspired dynamic 3d discriminative skeletal features for human action recognition," in *CVPRW*.
- [193] E. Ohn-Bar and M. Trivedi, "Joint angles similarities and hog2 for action recognition," in *CVPRW*.
- [194] G. T. Papadopoulos, A. Axenopoulos, and P. Daras, "Real-time skeleton-tracking-based human action recognition using kinect data," in *ICMM*.
- [195] H. Pazhoumand-Dar, C.-P. Lam, and M. Masek, "Joint movement similarities for robust 3d action recognition using skeletal data," *Vis. Commun. and Image Represent.*, vol. 30.
- [196] A. S. Keceli and A. B. Can, "Recognition of basic human actions using depth information," *Int. Jour. of Pattern Recognit. and Artificial Inte.*, vol. 28, no. 02.
- [197] W. Zhu, C. Lan, J. Xing, W. Zeng, Y. Li, L. Shen, and X. Xie, "Co-occurrence feature learning for skeleton based action recognition using regularized deep lstm networks," in *AAAI*, 2016.
- [198] C. Caetano, J. Sena, F. Brémond, J. A. Dos Santos, and W. R. Schwartz, "Skelemotion: A new representation of skeleton joint sequences based on motion information for 3d action recognition," in *AVSS*.
- [199] V. Veeriah, N. Zhuang, and G.-J. Qi, "Differential recurrent neural networks for action recognition," in *ICCV*.
- [200] Y. Du, W. Wang, and L. Wang, "Hierarchical recurrent neural network for skeleton based action recognition," in *CVPR*.
- [201] S. Zhang, X. Liu, and J. Xiao, "On geometric features for skeleton-based action recognition using multilayer lstm networks," in *WACV*.
- [202] H. Wang and L. Wang, "Modeling temporal dynamics and spatial configurations of actions using two-stream recurrent neural networks," in *CVPR*.
- [203] S. Song, C. Lan, J. Xing, W. Zeng, and J. Liu, "An end-to-end spatio-temporal attention model for human action recognition from skeleton data," in *AAAI*, 2017.
- [204] J. Liu, G. Wang, P. Hu, L.-Y. Duan, and A. C. Kot, "Global context-aware attention lstm networks for 3d action recognition," in *CVPR*.
- [205] I. Lee, D. Kim, S. Kang, and S. Lee, "Ensemble deep learning for skeleton-based action recognition using temporal sliding lstm networks," in *ICCV*.
- [206] P. Zhang, C. Lan, J. Xing, W. Zeng, J. Xue, and N. Zheng, "View adaptive recurrent neural networks for high performance human action recognition from skeleton data," in *ICCV*.
- [207] C. Xie, C. Li, B. Zhang, C. Chen, J. Han, C. Zou, and J. Liu, "Memory attention networks for skeleton-based action recognition," *arXiv preprint arXiv:1804.08254*, 2018.
- [208] S. Li, W. Li, C. Cook, Y. Gao, and C. Zhu, "Deep independently recurrent neural network (indrnn)," *arXiv preprint arXiv:1910.06251*, 2019.
- [209] Y. Du, Y. Fu, and L. Wang, "Skeleton based action recognition with convolutional neural network," in *ACPR*.
- [210] Y. Hou, Z. Li, P. Wang, and W. Li, "Skeleton optical spectra-based action recognition using convolutional neural networks," *TCSVT*, vol. 28, no. 3.
- [211] P. Wang, Z. Li, Y. Hou, and W. Li, "Action recognition based on joint trajectory maps using convolutional neural networks," in *ACM Multimedia*.
- [212] T. S. Kim and A. Reiter, "Interpretable 3d human action analysis with temporal convolutional networks," in *CVPRW*.
- [213] Q. Ke, S. An, M. Bennamoun, F. Sohel, and F. Boussaid, "Skeleton-net: Mining deep part features for 3-d action recognition," *IEEE signal process. lett.*, vol. 24, no. 6.
- [214] C. Li, Y. Hou, P. Wang, and W. Li, "Joint distance maps based action recognition with convolutional neural networks," *IEEE Signal Process. Lett.*, vol. 24, no. 5.
- [215] Q. Ke, M. Bennamoun, S. An, F. Sohel, and F. Boussaid, "A new representation of skeleton sequences for 3d action recognition," in *CVPR*.
- [216] M. Liu, H. Liu, and C. Chen, "Enhanced skeleton visualization for view invariant human action recognition," *Pattern Recognition*, vol. 68.
- [217] B. Li, Y. Dai, X. Cheng, H. Chen, Y. Lin, and M. He, "Skeleton based action recognition using translation-scale invariant image mapping and multi-scale deep cnn," in *ICMEW*.
- [218] Q. Ke, M. Bennamoun, S. An, F. Sohel, and F. Boussaid, "Learning clip representations for skeleton-based 3d action recognition," *TIP*, vol. 27, no. 6.
- [219] Y. Xu, J. Cheng, L. Wang, H. Xia, F. Liu, and D. Tao, "Ensemble one-dimensional convolution neural networks for skeleton-based action recognition," *IEEE Signal Process. Lett.*, vol. 25, no. 7.
- [220] C. Li, Q. Zhong, D. Xie, and S. Pu, "Co-occurrence feature learning from skeleton data for action recognition and detection with hierarchical aggregation," *arXiv preprint arXiv:1804.06055*, 2018.
- [221] F. Yang, Y. Wu, S. Sakti, and S. Nakamura, "Make skeleton-based action recognition model smaller, faster and better," in *ACM Multimedia Asia*.
- [222] C. Caetano, F. Brémond, and W. R. Schwartz, "Skeleton image representation for 3d action recognition based on tree structure and reference joints," in *SIBGRAPI*.
- [223] J. Liu, N. Akhtar, and A. Mian, "Skepxels: Spatio-temporal image representation of human skeleton joints for action recognition," in *CVPRW*, 2019.
- [224] Y. Li, R. Xia, X. Liu, and Q. Huang, "Learning shape-motion representations from geometric algebra spatio-temporal model for skeleton-based action recognition," in *ICME*.

- [225] P. Zhang, C. Lan, J. Xing, W. Zeng, J. Xue, and N. Zheng, "View adaptive neural networks for high performance skeleton-based human action recognition," *TPAMI*, vol. 41, no. 8.
- [226] A. Banerjee, P. K. Singh, and R. Sarkar, "Fuzzy integral based cnn classifier fusion for 3d skeleton action recognition," *TCSVT*, 2020.
- [227] A. Zhu, Q. Wu, R. Cui, T. Wang, W. Hang, G. Hua, and H. Snoussi, "Exploring a rich spatial-temporal dependent relational model for skeleton-based action recognition by bidirectional lstm-cnn," *Neurocomputing*, vol. 414.
- [228] C. Si, Y. Jing, W. Wang, L. Wang, and T. Tan, "Skeleton-based action recognition with spatial reasoning and temporal stack learning," in *ECCV*.
- [229] L. Shi, Y. Zhang, J. Cheng, and H. Lu, "Skeleton-based action recognition with directed graph neural networks," in *CVPR*.
- [230] M. Li, S. Chen, Y. Zhao, Y. Zhang, Y. Wang, and Q. Tian, "Dynamic multiscale graph neural networks for 3d skeleton based human motion prediction," in *CVPR*.
- [231] Y. Tang, Y. Tian, J. Lu, P. Li, and J. Zhou, "Deep progressive reinforcement learning for skeleton-based action recognition," in *CVPR*.
- [232] Y.-H. Wen, L. Gao, H. Fu, F.-L. Zhang, and S. Xia, "Graph cnns with motif and variable temporal block for skeleton-based action recognition," in *AAAI*, vol. 33.
- [233] X. Zhang, C. Xu, X. Tian, and D. Tao, "Graph edge convolutional neural networks for skeleton-based action recognition," *TNNLS*, 2019.
- [234] M. Li, S. Chen, X. Chen, Y. Zhang, Y. Wang, and Q. Tian, "Actional-structural graph convolutional networks for skeleton-based action recognition," in *CVPR*.
- [235] B. Li, X. Li, Z. Zhang, and F. Wu, "Spatio-temporal graph routing for skeleton-based action recognition," in *AAAI*, vol. 33.
- [236] L. Shi, Y. Zhang, J. Cheng, and H. Lu, "Two-stream adaptive graph convolutional networks for skeleton-based action recognition," in *CVPR*.
- [237] C. Si, W. Chen, W. Wang, L. Wang, and T. Tan, "An attention enhanced graph convolutional lstm network for skeleton-based action recognition," in *CVPR*.
- [238] C. Wu, X.-J. Wu, and J. Kittler, "Spatial residual layer and dense connection block enhanced spatial temporal graph convolutional network for skeleton-based action recognition," in *ICCVW*.
- [239] X. Zhang, C. Xu, and D. Tao, "Context aware graph convolution for skeleton-based action recognition," in *CVPR*.
- [240] P. Zhang, C. Lan, W. Zeng, J. Xing, J. Xue, and N. Zheng, "Semantics-guided neural networks for efficient skeleton-based human action recognition," in *CVPR*.
- [241] W. Peng, X. Hong, H. Chen, and G. Zhao, "Learning graph convolutional network for skeleton-based human action recognition by neural searching," in *AAAI*.
- [242] K. Cheng, Y. Zhang, X. He, W. Chen, J. Cheng, and H. Lu, "Skeleton-based action recognition with shift graph convolutional network," in *CVPR*.
- [243] Z. Liu, H. Zhang, Z. Chen, Z. Wang, and W. Ouyang, "Disentangling and unifying graph convolutions for skeleton-based action recognition," in *CVPR*.
- [244] J. Liu, G. Wang, L.-Y. Duan, K. Abdiyeva, and A. C. Kot, "Skeleton-based human action recognition with global context-aware attention lstm networks," *TIP*, vol. 27, no. 4.
- [245] J. Liu, A. Shahroudy, D. Xu, and G. Wang, "Spatio-temporal lstm with trust gates for 3d human action recognition," in *ECCV*.
- [246] S. Zhang, Y. Yang, J. Xiao, X. Liu, Y. Yang, D. Xie, and Y. Zhuang, "Fusing geometric features for skeleton-based action recognition using multilayer lstm networks," *TMM*, vol. 20, no. 9.
- [247] L. Zhao, Y. Song, C. Zhang, Y. Liu, P. Wang, T. Lin, M. Deng, and H. Li, "T-gcn: A temporal graph convolutional network for traffic prediction," *IEEE trans. Intell. Transp. Syst.*, 2019.
- [248] F. Monti, K. Otness, and M. M. Bronstein, "Motifnet: a motif-based graph convolutional network for directed graphs," in *DSW*.
- [249] H. Mohaghegh, N. Karimi, R. Soroushmehr, S. Samavi, and K. Najarian, "Aggregation of rich depth aware features in a modified stacked generalization model for single image depth estimation," *TCSVT*, vol. 29.
- [250] M. Harville and D. Li, "Fast, integrated person tracking and activity recognition with plan-view templates from a single stereo camera," in *CVPR*, vol. 2.
- [251] M.-C. Roh, H.-K. Shin, and S.-W. Lee, "View-independent human action recognition with volume motion template on single stereo camera," *Pattern Recognition Letters*, vol. 31, no. 7.
- [252] H. Rahmani, A. Mahmood, D. Q. Huynh, and A. Mian, "Real time action recognition using histograms of depth gradients and random decision forests," in *WACV*.
- [253] X. Yang and Y. Tian, "Super normal vector for activity recognition using depth sequences," in *CVPR*.
- [254] W. Li, Z. Zhang, and Z. Liu, "Action recognition based on a bag of 3d points," in *CVPRW*.
- [255] A. W. Vieira, E. R. Nascimento, G. L. Oliveira, Z. Liu, and M. F. Campos, "Stop: Space-time occupancy patterns for 3d action recognition from depth map sequences," in *CIARP*.
- [256] J. Wang, Z. Liu, J. Chorowski, Z. Chen, and Y. Wu, "Robust 3d action recognition with random occupancy patterns," in *ECCV*.
- [257] L. Xia and J. Aggarwal, "Spatio-temporal depth cuboid similarity feature for activity recognition using depth camera," in *CVPR*.
- [258] C. Lu, J. Jia, and C.-K. Tang, "Range-sample depth feature for action recognition," in *CVPR*.
- [259] X. Yang, C. Zhang, and Y. Tian, "Recognizing actions using depth motion maps-based histograms of oriented gradients," in *ACM Multimedia*.
- [260] W. Chen and G. Guo, "Triviews: A general framework to use 3d depth data effectively for action recognition," *Vis. Commun. Image Represent.*, vol. 26.
- [261] C. Chen, K. Liu, and N. Kehtarnavaz, "Real-time human action recognition based on depth motion maps," *JRTIP*, vol. 12, no. 1.
- [262] C. Chen, R. Jafari, and N. Kehtarnavaz, "Action recognition from depth sequences using depth motion maps-based local binary patterns," in *WACV*.
- [263] O. Oreifej and Z. Liu, "Hon4d: Histogram of oriented 4d normals for activity recognition from depth sequences," in *CVPR*.
- [264] P. Wang, S. Wang, Z. Gao, Y. Hou, and W. Li, "Structured images for rgb-d action recognition," in *ICCVW*.
- [265] P. Wang, W. Li, Z. Gao, J. Zhang, C. Tang, and P. O. Ogunbona, "Action recognition from depth maps using deep convolutional neural networks," *IEEE Trans. Hum. Mach. Syst.*, vol. 46, no. 4.
- [266] C. Chen, M. Liu, B. Zhang, J. Han, J. Jiang, and H. Liu, "3d action recognition using multi-temporal depth motion maps and fisher vector," in *IJCAI*.
- [267] B. Fernando, E. Gavves, J. Oramas, A. Ghodrati, and T. Tuytelaars, "Rank pooling for action recognition," *TPAMI*, vol. 39, no. 4.
- [268] P. Wang, W. Li, Z. Gao, C. Tang, and P. O. Ogunbona, "Depth pooling based large-scale 3-d action recognition with convolutional neural networks," *TMM*, vol. 20, no. 5.
- [269] Y. Zhu and S. Newsam, "Depth2action: Exploring embedded depth for large-scale action recognition," in *ECCV*.
- [270] Y. Xiao, J. Chen, Y. Wang, Z. Cao, J. T. Zhou, and X. Bai, "Action recognition for depth video using multi-view dynamic images," *Information Sciences*, vol. 480.
- [271] A. Sanchez-Caballero, S. de López-Diz, D. Fuentes-Jimenez, C. Losada-Gutiérrez, M. Marrón-Romera, D. Casillas-Perez, and M. I. Sarker, "3dfcnn: Real-time action recognition using 3d deep neural networks with raw depth information," *arXiv preprint arXiv:2006.07743*, 2020.
- [272] A. Sanchez-Caballero, D. Fuentes-Jimenez, and C. Losada-Gutiérrez, "Exploiting the convlstm: Human action recognition using raw depth video-based recurrent neural networks," *arXiv preprint arXiv:2006.07744*, 2020.
- [273] J. Han and B. Bhanu, "Human activity recognition in thermal infrared imagery," in *CVPRW*.
- [274] S. Ali and N. Bouguila, "Variational learning of beta-liouville hidden markov models for infrared action recognition," in *CVPRW*.
- [275] Z. Xue, D. Ming, W. Song, B. Wan, and S. Jin, "Infrared gait recognition based on wavelet transform and support vector machine," *Pattern recognition*, vol. 43, no. 8.
- [276] H. Eum, J. Lee, C. Yoon, and M. Park, "Human action recognition for night vision using temporal templates with infrared thermal camera," in *URAI*.
- [277] T. Kawashima, Y. Kawanishi, I. Ide, H. Murase, D. Deguchi, T. Aizawa, and M. Kawade, "Action recognition from extremely low-resolution thermal image sequence," in *AVSS*.
- [278] A. K. Shah, R. Ghosh, and A. Akula, "A spatio-temporal deep learning approach for human action recognition in infrared videos," in *Optics and Photonics for Information Processing XII*, vol. 10751.

- [279] H. Megloul, L. Bentabet, M. Airouche, *et al.*, "A new technique based on 3d convolutional neural networks and filtering optical flow maps for action classification in infrared video," *Control Eng. Appl. Inf.*, vol. 21, no. 4.
- [280] A. Akula, A. K. Shah, and R. Ghosh, "Deep learning approach for human action recognition in infrared images," *Cognitive Systems Research*, vol. 50.
- [281] I. Morawski and W.-N. Lie, "Two-stream deep learning architecture for action recognition by using extremely low-resolution infrared thermopile arrays," in *IWAIT*, vol. 11515.
- [282] Y. Liu, Z. Lu, J. Li, T. Yang, and C. Yao, "Global temporal representation based cnns for infrared action recognition," *IEEE Signal Processing Letters*, vol. 25, no. 6.
- [283] J. Imran and B. Raman, "Deep residual infrared action recognition by integrating local and global spatio-temporal cues," *Infrared Physics & Technology*, vol. 102.
- [284] J. Imran and B. Raman, "Evaluating fusion of rgb-d and inertial sensors for multimodal human action recognition," *JAIHC*, vol. 11, no. 1.
- [285] V. Mehta, A. Dhall, S. Pal, and S. Khan, "Motion and region aware adversarial learning for fall detection with thermal imaging," *arXiv preprint arXiv:2004.08352*, 2020.
- [286] R. B. Rusu, J. Bandouch, Z. C. Marton, N. Blodow, and M. Beetz, "Action recognition in intelligent environments using point cloud features extracted from silhouette sequences," in *RO-MAN*.
- [287] M. Bregonzio, S. Gong, and T. Xiang, "Recognising action as clouds of space-time interest points," in *CVPR*.
- [288] M. Munaro, G. Ballin, S. Michieletto, and E. Menegatti, "3d flow estimation for human action recognition from colored point clouds," *BICA*, vol. 5.
- [289] H. Rahmani, A. Mahmood, D. Q. Huynh, and A. Mian, "Hopc: Histogram of oriented principal components of 3d pointclouds for action recognition," in *ECCV*.
- [290] H. Rahmani, A. Mahmood, D. Huynh, and A. Mian, "Histogram of oriented principal components for cross-view action recognition," *TPAMI*, vol. 38, no. 12.
- [291] M. Khokhlova, C. Migniot, and A. Dipanda, "3d point cloud descriptor for posture recognition," in *VISIGRAPP*.
- [292] C. R. Qi, L. Yi, H. Su, and L. J. Guibas, "Pointnet++: Deep hierarchical feature learning on point sets in a metric space," in *NeurIPS*.
- [293] S. U. Innocenti, F. Becattini, F. Pernici, and A. Del Bimbo, "Temporal binary representation for event-based action recognition," *arXiv preprint arXiv:2010.08946*, 2020.
- [294] P. Lichtsteiner, C. Posch, and T. Delbruck, "A $128 \times 128 \times 120$ db 15 μ s latency asynchronous temporal contrast vision sensor," *IEEE journal of solid-state circuits*, vol. 43, no. 2.
- [295] R. Berner, C. Brandli, M. Yang, S.-C. Liu, and T. Delbruck, "A 240×180 10mw 12us latency sparse-output vision sensor for mobile applications," in *Symposium on VLSI Circuits*.
- [296] S. A. Baby, B. Vinod, C. Chinni, and K. Mitra, "Dynamic vision sensors for human activity recognition," in *ACPR*.
- [297] X. Clady, J.-M. Maro, S. Barré, and R. B. Benosman, "A motion-based feature for event-based pattern recognition," *Frontiers in neuroscience*, vol. 10.
- [298] R. Ghosh, A. Gupta, A. Nakagawa, A. Soares, and N. Thakor, "Spatiotemporal filtering for event-based action recognition," *arXiv preprint arXiv:1903.07067*, 2019.
- [299] C. Huang, "Event-based action recognition using timestamp image encoding network," *arXiv preprint arXiv:2009.13049*, 2020.
- [300] Y. Bi, A. Chadha, A. Abbas, E. Boursoulatzé, and Y. Andreopoulos, "Graph-based spatio-temporal feature learning for neuro-morphic vision sensing," *TIP*, vol. 29.
- [301] A. Amir, B. Taba, D. Berg, T. Melano, J. McKinstry, C. Di Nolfo, T. Nayak, A. Andreopoulos, G. Garreau, M. Mendoza, *et al.*, "A low power, fully event-based gesture recognition system," in *CVPR*.
- [302] Q. Wang, Y. Zhang, J. Yuan, and Y. Lu, "Space-time event clouds for gesture recognition: from rgb cameras to event cameras," in *WACV*.
- [303] J. Chen, J. Meng, X. Wang, and J. Yuan, "Dynamic graph cnn for event-camera based gesture recognition," in *ISCAS*.
- [304] A. M. George, D. Banerjee, S. Dey, A. Mukherjee, and P. Balamurali, "A reservoir-based convolutional spiking neural network for gesture recognition from dvs input," in *IJCNN*.
- [305] A. Chadha, Y. Bi, A. Abbas, and Y. Andreopoulos, "Neuromorphic vision sensing for cnn-based action recognition," in *ICASSP*.
- [306] C. Hori, T. Hori, T.-Y. Lee, Z. Zhang, B. Harsham, J. R. Hershey, T. K. Marks, and K. Sumi, "Attention-based multimodal fusion for video description," in *ICCV*.
- [307] Q. Wu, Z. Wang, F. Deng, Z. Chi, and D. D. Feng, "Realistic human action recognition with multimodal feature selection and fusion," *IEEE T. Syst. Man. CY-S*, vol. 43, no. 4.
- [308] C. Wang, H. Yang, and C. Meinel, "Exploring multimodal video representation for action recognition," in *IJCNN*.
- [309] R. Arandjelovic and A. Zisserman, "Look, listen and learn," in *ICCV*.
- [310] B. Korbar, D. Tran, and L. Torresani, "Cooperative learning of audio and video models from self-supervised synchronization," in *NeurIPS*.
- [311] A. Owens and A. A. Efros, "Audio-visual scene analysis with self-supervised multisensory features," in *ECCV*.
- [312] P. Casale, O. Pujol, and P. Radeva, "Human activity recognition from accelerometer data using a wearable device," in *ibPRIA*.
- [313] A. Bayat, M. Pomplun, and D. A. Tran, "A study on human activity recognition using accelerometer data from smartphones," *Procedia Computer Science*, vol. 34.
- [314] A. M. Khan, Y.-K. Lee, S.-Y. Lee, and T.-S. Kim, "Human activity recognition via an accelerometer-enabled-smartphone using kernel discriminant analysis," in *FutureTech*.
- [315] U. Maurer, A. Smailagic, D. P. Siewiorek, and M. Deisher, "Activity recognition and monitoring using multiple sensors on different body positions," in *BSN*.
- [316] J. Mantyjarvi, J. Himberg, and T. Seppanen, "Recognizing human motion with multiple acceleration sensors," in *SMC*, vol. 2.
- [317] L. Bao and S. S. Intille, "Activity recognition from user-annotated acceleration data," in *Int. conf. pervasive comput.*
- [318] N. Ravi, N. Dandekar, P. Mysore, and M. L. Littman, "Activity recognition from accelerometer data," in *AAAI*, vol. 5.
- [319] J. Lester, T. Choudhury, and G. Borriello, "A practical approach to recognizing physical activities," in *PerCom*.
- [320] A. Mannini and A. M. Sabatini, "Machine learning methods for classifying human physical activity from on-body accelerometers," *Sensors*, vol. 10, no. 2.
- [321] K. Altun and B. Barshan, "Human activity recognition using inertial/magnetic sensor units," in *HBUW*.
- [322] D. Anguita, A. Ghio, L. Oneto, X. Parra, and J. L. Reyes-Ortiz, "A public domain dataset for human activity recognition using smartphones," in *ESANN*, vol. 3.
- [323] W. Jiang and Z. Yin, "Human activity recognition using wearable sensors by deep convolutional neural networks," in *ACM Multimedia*.
- [324] F. J. Ordóñez and D. Roggen, "Deep convolutional and lstm recurrent neural networks for multimodal wearable activity recognition," *Sensors*, vol. 16, no. 1.
- [325] A. Ignatov, "Real-time human activity recognition from accelerometer data using convolutional neural networks," *Applied Soft Computing*, vol. 62.
- [326] H. Fan, C. Luo, C. Zeng, M. Ferienc, Z. Que, S. Liu, X. Niu, and W. Luk, "F-e3d: Fpga-based acceleration of an efficient 3d convolutional neural network for human action recognition," in *ASAP*, vol. 2160.
- [327] A. Lin and H. Ling, "Doppler and direction-of-arrival (ddoa) radar for multiple-mover sensing," *IEEE trans. Aero. Elec. Sys.*, vol. 43, no. 4.
- [328] A. Stove, "Modern fmcw radar-techniques and applications," in *EURAD*.
- [329] Y. Kim and H. Ling, "Human activity classification based on micro-doppler signatures using a support vector machine," *TGRS*, vol. 47, no. 5.
- [330] P. Van Dorp and F. Groen, "Feature-based human motion parameter estimation with radar," *IET Radar, Sonar & Navigation*, vol. 2, no. 2.
- [331] D. Tahmoush and J. Silvius, "Radar micro-doppler for long range front-view gait recognition," in *BTAS*.
- [332] J. Park, R. J. Javier, T. Moon, and Y. Kim, "Micro-doppler based classification of human aquatic activities via transfer learning of convolutional neural networks," *Sensors*, vol. 16, no. 12.
- [333] R. Trommel, R. Harmanny, L. Cifola, and J. Driessen, "Multi-target human gait classification using deep convolutional neural networks on micro-doppler spectrograms," in *EuRAD*.
- [334] S. A. Shah and F. Fioranelli, "Human activity recognition: preliminary results for dataset portability using fmcw radar," in *RADAR*.

- [335] M. S. Seyfioğlu, A. M. Özbayoğlu, and S. Z. Gürbüz, "Deep convolutional autoencoder for radar-based classification of similar aided and unaided human activities," *IEEE Trans. Aero. Elec. Sys.*, vol. 54, no. 4.
- [336] B. Vandersmissen, N. Knudde, A. Jalalvand, I. Couckuyt, A. Bourdoux, W. De Neve, and T. Dhaene, "Indoor person identification using a low-power fmcw radar," *TGRS*, vol. 56, no. 7.
- [337] M. Wang, Y. D. Zhang, and G. Cui, "Human motion recognition exploiting radar with stacked recurrent neural network," *Digital Signal Processing*, vol. 87.
- [338] S. Yang, J. Le Kerneec, and F. Fioranelli, "Action recognition using indoor radar systems," *IET Human Motion Analysis for Healthcare Applications*, 2019.
- [339] H. Zou, J. Yang, H. Prasanna Das, H. Liu, Y. Zhou, and C. J. Spanos, "Wifi and vision multimodal learning for accurate and robust device-free human activity recognition," in *CVPRW*.
- [340] W. Wang, A. X. Liu, M. Shahzad, K. Ling, and S. Lu, "Device-free human activity recognition using commercial wifi devices," *J-SAC*, vol. 35, no. 5.
- [341] W. Wang, A. X. Liu, and M. Shahzad, "Gait recognition using wifi signals," in *UbiComp*.
- [342] G. Wang, Y. Zou, Z. Zhou, K. Wu, and L. M. Ni, "We can hear you with wi-fi!," *IEEE Trans. Mob. Comput.*, vol. 15, no. 11.
- [343] S. Duan, T. Yu, and J. He, "Widriver: Driver activity recognition system based on wifi csi," *Int. J. Wirel. Inf. Netw.*, vol. 25, no. 2.
- [344] Y. Wang, K. Wu, and L. M. Ni, "Wifall: Device-free fall detection by wireless networks," *IEEE Trans. Mob. Comput.*, vol. 16, no. 2.
- [345] F. Wang, Y. Song, J. Zhang, J. Han, and D. Huang, "Temporal unet: Sample level human action recognition using wifi," *arXiv preprint arXiv:1904.11953*, 2019.
- [346] Q. Kong, Z. Wu, Z. Deng, M. Klinkigt, B. Tong, and T. Murakami, "Mmact: A large-scale dataset for cross modal human action understanding," in *ICCV*.
- [347] C. Chen, R. Jafari, and N. Kehtarnavaz, "Utd-mhad: A multimodal dataset for human action recognition utilizing a depth camera and a wearable inertial sensor," in *ICIP*.
- [348] J. Yang, J. Lee, and J. Choi, "Activity recognition based on rfid object usage for smart mobile devices," *JCST*, vol. 26, no. 2.
- [349] T. Li, L. Fan, M. Zhao, Y. Liu, and D. Katabi, "Making the invisible visible: Action recognition through walls and occlusions," in *ICCV*.
- [350] W. Xu, G. Lan, Q. Lin, S. Khalifa, N. Bergmann, M. Hassan, and W. Hu, "Keh-gait: Towards a mobile healthcare user authentication system by kinetic energy harvesting," in *NDSS*, no. 0.2.
- [351] D. Ma, G. Lan, W. Xu, M. Hassan, and W. Hu, "Simultaneous energy harvesting and gait recognition using piezoelectric energy harvester," *arXiv preprint arXiv:2009.02752*, 2020.
- [352] Y. Wang, B. Du, Y. Shen, K. Wu, G. Zhao, J. Sun, and H. Wen, "Ev-gait: Event-based robust gait recognition using dynamic vision sensors," in *CVPR*.
- [353] A. Nagrani, C. Sun, D. Ross, R. Sukthankar, C. Schmid, and A. Zisserman, "Speech2action: Cross-modal supervision for action recognition," in *CVPR*.
- [354] T. Baltrušaitis, C. Ahuja, and L.-P. Morency, "Multimodal machine learning: A survey and taxonomy," *TPAMI*, vol. 41, no. 2.
- [355] Y. Zhao, Z. Liu, L. Yang, and H. Cheng, "Combing rgb and depth map features for human activity recognition," in *APSIPA ASC*.
- [356] L. Liu and L. Shao, "Learning discriminative representations from rgb-d video data," in *IJCAI*, 2013.
- [357] Y. Kong and Y. Fu, "Bilinear heterogeneous information machine for rgb-d action recognition," in *CVPR*.
- [358] Y. Kong and Y. Fu, "Max-margin heterogeneous information machine for rgb-d action recognition," *IJCV*, vol. 123, no. 3.
- [359] J. Imran and P. Kumar, "Human action recognition using rgb-d sensor and deep convolutional neural networks," in *ICACCI*.
- [360] P. Wang, W. Li, Z. Gao, Y. Zhang, C. Tang, and P. Ogunbona, "Scene flow to action map: A new representation for rgb-d based action recognition with convolutional neural networks," in *CVPR*.
- [361] L. Wang, Z. Ding, Z. Tao, Y. Liu, and Y. Fu, "Generative multi-view human action recognition," in *ICCV*.
- [362] C. Dhiman and D. K. Vishwakarma, "View-invariant deep architecture for human action recognition using two-stream motion and shape temporal dynamics," *TIP*, vol. 29.
- [363] H. Wang, Z. Song, W. Li, and P. Wang, "A hybrid network for large-scale action recognition from rgb and depth modalities," *Sensors*, vol. 20, no. 11.
- [364] A. Shahroudy, G. Wang, and T.-T. Ng, "Multi-modal feature fusion for action recognition in rgb-d sequences," in *ISCCSP*.
- [365] A. Franco, A. Magnani, and D. Maio, "A multimodal approach for human activity recognition based on skeleton and rgb data," *Pattern Recognition Letters*, vol. 131.
- [366] A. Shahroudy, T.-T. Ng, Y. Gong, and G. Wang, "Deep multimodal feature analysis for action recognition in rgb+ d videos," *TPAMI*, vol. 40, no. 5.
- [367] M. Zolfaghari, G. L. Oliveira, N. Sedaghat, and T. Brox, "Chained multi-stream networks exploiting pose, motion, and appearance for action classification and detection," in *ICCV*.
- [368] R. Zhao, H. Ali, and P. Van der Smagt, "Two-stream rnn/cnn for action recognition in 3d videos," in *IROS*.
- [369] F. Baradel, C. Wolf, and J. Mille, "Pose-conditioned spatio-temporal attention for human action recognition," *arXiv preprint arXiv:1703.10106*, 2017.
- [370] J. Liu, Y. Li, S. Song, J. Xing, C. Lan, and W. Zeng, "Multi-modality multi-task recurrent neural network for online action detection," *TCSVT*, vol. 29, no. 9.
- [371] S. Song, C. Lan, J. Xing, W. Zeng, and J. Liu, "Skeleton-indexed deep multi-modal feature learning for high performance human action recognition," in *ICME*.
- [372] J.-F. Hu, W.-S. Zheng, J. Lai, and J. Zhang, "Jointly learning heterogeneous features for rgb-d activity recognition," in *CVPR*.
- [373] J. Ye, K. Li, G.-J. Qi, and K. A. Hua, "Temporal order-preserving dynamic quantization for human action recognition from multimodal sensor streams," in *ACM Multimedia*.
- [374] J. Kong, T. Liu, and M. Jiang, "Collaborative multimodal feature learning for rgb-d action recognition," *J. Vis. Commun. Image Represent.*, vol. 59.
- [375] A. Chaaraoui, J. Padilla-Lopez, and F. Flórez-Revuelta, "Fusion of skeletal and silhouette-based features for human action recognition with rgb-d devices," in *ICCVW*.
- [376] S. Althloothi, M. H. Mahoor, X. Zhang, and R. M. Voyles, "Human activity recognition using multi-features and multiple kernel learning," *Pattern recognition*, vol. 47, no. 5.
- [377] A. Shahroudy, T.-T. Ng, Q. Yang, and G. Wang, "Multimodal multi-part learning for action recognition in depth videos," *TPAMI*, vol. 38, no. 10.
- [378] A. Jalal, Y.-H. Kim, Y.-J. Kim, S. Kamal, and D. Kim, "Robust human activity recognition from depth video using spatiotemporal multi-fused features," *Pattern recognition*, vol. 61.
- [379] Z. Shi and T.-K. Kim, "Learning and refining of privileged information-based rnns for action recognition from depth sequences," in *CVPR*.
- [380] H. Rahmani and M. Bennamoun, "Learning action recognition model from depth and skeleton videos," in *ICCV*.
- [381] A. Kamel, B. Sheng, P. Yang, P. Li, R. Shen, and D. D. Feng, "Deep convolutional neural networks for human action recognition using depth maps and postures," *IEEE Trans. Syst. Man Cybern. Syst.*, vol. 49, no. 9.
- [382] C. Zhao, M. Chen, J. Zhao, Q. Wang, and Y. Shen, "3d behavior recognition based on multi-modal deep space-time learning," *Applied Sciences*, vol. 9, no. 4.
- [383] C. Chen, R. Jafari, and N. Kehtarnavaz, "Improving human action recognition using fusion of depth camera and inertial sensors," *IEEE Trans. Hum. Mach. Syst.*, vol. 45, no. 1.
- [384] C. Chen, R. Jafari, and N. Kehtarnavaz, "A real-time human action recognition system using depth and inertial sensor fusion," *IEEE Sensors Journal*, vol. 16, no. 3.
- [385] Q. Zou, L. Ni, Q. Wang, Q. Li, and S. Wang, "Robust gait recognition by integrating inertial and rgbd sensors," *IEEE trans. cybern.*, vol. 48, no. 4.
- [386] N. E. D. Elmadany, Y. He, and L. Guan, "Multimodal learning for human action recognition via bimodal/multimodal hybrid centroid canonical correlation analysis," *TMM*, vol. 21, no. 5.
- [387] F. Malawski and B. Kwolek, "Improving multimodal action representation with joint motion history context," *J. Vis. Commun. Image Represent.*, vol. 61.
- [388] M. Ehatisham-Ul-Haq, A. Javed, M. A. Azam, H. M. Malik, A. Irtaza, I. H. Lee, and M. T. Mahmood, "Robust human activity recognition using multimodal feature-level fusion," *IEEE Access*, vol. 7.

- [389] R. Memmesheimer, N. Theisen, and D. Paulus, "Gimme signals: Discriminative signal encoding for multimodal activity recognition," *arXiv preprint arXiv:2003.06156*, 2020.
- [390] A. M. de Boissiere and R. Noumeir, "Infrared and 3d skeleton feature fusion for rgb-d action recognition," *arXiv preprint arXiv:2002.12886*, 2020.
- [391] Q. Zou, Y. Wang, Q. Wang, Y. Zhao, and Q. Li, "Deep learning-based gait recognition using smartphones in the wild," *IEEE Trans. Inf. Forens. Sec.*, vol. 15.
- [392] J. Liu, A. Shahroudy, G. Wang, L.-Y. Duan, and A. C. Kot, "Skeleton-based online action prediction using scale selection network," *TPAMI*, vol. 42, no. 6.
- [393] L. Wang, C. Gao, L. Yang, Y. Zhao, W. Zuo, and D. Meng, "Pm-gans: Discriminative representation learning for action recognition using partial-modalities," in *ECCV*.
- [394] F. M. Thoker and J. Gall, "Cross-modal knowledge distillation for action recognition," in *ICIP*.
- [395] N. C. Garcia, P. Morerio, and V. Murino, "Modality distillation with multiple stream networks for action recognition," in *ECCV*.
- [396] C. Jia, Z. Ding, Y. Kong, and Y. Fu, "Semi-supervised cross-modality action recognition by latent tensor transfer learning," *TCSVT*, 2019.
- [397] S. Song, J. Liu, Y. Li, and Z. Guo, "Modality compensation network: Cross-modal adaptation for action recognition," *TIP*, vol. 29.
- [398] Y. Aytar, C. Vondrick, and A. Torralba, "Soundnet: Learning sound representations from unlabeled video," in *NeurIPS*.
- [399] H. Alwassel, D. Mahajan, L. Torresani, B. Ghanem, and D. Tran, "Self-supervised learning by cross-modal audio-video clustering," *arXiv preprint arXiv:1911.12667*, 2019.
- [400] A. Perez, V. Sanguineti, P. Morerio, and V. Murino, "Audio-visual model distillation using acoustic images," in *WACV*.
- [401] F. Caba Heilbron, V. Escorcia, B. Ghanem, and J. Carlos Niebles, "Activitynet: A large-scale video benchmark for human activity understanding," in *CVPR*.
- [402] C. Schuldt, I. Laptev, and B. Caputo, "Recognizing human actions: a local svm approach," in *ICPR*, vol. 3.
- [403] M. Müller, T. Röder, M. Clausen, B. Eberhardt, B. Krüger, and A. Weber, "Documentation mocap database hdm05," 2007.
- [404] M. Marszalek, I. Laptev, and C. Schmid, "Actions in context," in *CVPR*.
- [405] J. C. Niebles, C.-W. Chen, and L. Fei-Fei, "Modeling temporal structure of decomposable motion segments for activity classification," in *ECCV*.
- [406] O. Kliper-Gross, T. Hassner, and L. Wolf, "The action similarity labeling challenge," *TPAMI*, vol. 34, no. 3.
- [407] J. Sung, C. Ponce, B. Selman, and A. Saxena, "Human activity detection from rgb-d images," in *AAAI*, 2011.
- [408] Z. Cheng, L. Qin, Y. Ye, Q. Huang, and Q. Tian, "Human daily action analysis with multi-view and color-depth data," in *ECCV*.
- [409] Y.-C. Lin, M.-C. Hu, W.-H. Cheng, Y.-H. Hsieh, and H.-M. Chen, "Human action recognition and retrieval using sole depth information," in *ACM Multimedia*.
- [410] K. K. Reddy and M. Shah, "Recognizing 50 human action categories of web videos," *Machine vision and applications*, vol. 24, no. 5.
- [411] H. S. Koppula, R. Gupta, and A. Saxena, "Learning human activities and object affordances from rgb-d videos," *Int. J. Rob. Res.*, vol. 32, no. 8.
- [412] H. Jhuang, J. Gall, S. Zuffi, C. Schmid, and M. J. Black, "Towards understanding action recognition," in *ICCV*.
- [413] C. Ellis, S. Z. Masood, M. F. Tappen, J. J. LaViola, and R. Sukthankar, "Exploring the trade-off between accuracy and observational latency in action recognition," *IJCV*, vol. 101, no. 3.
- [414] A.-A. Liu, Y.-T. Su, P.-P. Jia, Z. Gao, T. Hao, and Z.-X. Yang, "Multiple/single-view human action recognition via part-induced multitask structural learning," *IEEE Trans. Cybern.*, vol. 45, no. 6.
- [415] J. Wang, X. Nie, Y. Xia, Y. Wu, and S.-C. Zhu, "Cross-view action modeling, learning and recognition," in *CVPR*.
- [416] I. Theodorakopoulos, D. Kastaniotis, G. Economou, and S. Ftopoulos, "Pose-based human action recognition via sparse representation in dissimilarity space," *J. Vis. Commun. Image Represent.*, vol. 25, no. 1.
- [417] H. Rahmani, A. Mahmood, D. Huynh, and A. Mian, "Action classification with locality-constrained linear coding," in *ICPR*.
- [418] K. J. Piczak, "Esc: Dataset for environmental sound classification," in *ACM Multimedia*.
- [419] A.-A. Liu, W.-Z. Nie, Y.-T. Su, L. Ma, T. Hao, and Z.-X. Yang, "Coupled hidden conditional random fields for rgb-d human action recognition," *Signal Processing*, vol. 112.
- [420] S. Abu-El-Haija, N. Kothari, J. Lee, P. Natsev, G. Toderici, B. Varadarajan, and S. Vijayanarasimhan, "Youtube-8m: A large-scale video classification benchmark," *arXiv preprint arXiv:1609.08675*, 2016.
- [421] R. Goyal, S. E. Kahou, V. Michalski, J. Materzynska, S. Westphal, H. Kim, V. Haenel, I. Fruend, P. Yianilos, M. Mueller-Freitag, et al., "The "something something" video database for learning and evaluating visual common sense.," in *ICCV*, vol. 1.
- [422] C. Gu, C. Sun, D. A. Ross, C. Pantofaru, Y. Li, S. Vijayanarasimhan, G. Toderici, S. Ricco, R. Sukthankar, et al., "Ava: A video dataset of spatio-temporally localized atomic visual actions," in *CVPR*.
- [423] Y.-G. Jiang, Z. Wu, J. Wang, X. Xue, and S.-F. Chang, "Exploiting feature and class relationships in video categorization with regularized deep neural networks," *TPAMI*, vol. 40, no. 2.
- [424] D. Micucci, M. Mobilio, and P. Napolitano, "Unimib shar: A dataset for human activity recognition using acceleration data from smartphones," *Applied Sciences*, vol. 7, no. 10.
- [425] D. Damen, H. Doughty, G. Maria Farinella, S. Fidler, A. Furnari, E. Kazakos, D. Moltisanti, J. Munro, T. Perrett, W. Price, et al., "Scaling egocentric vision: The epic-kitchens dataset," in *ECCV*.
- [426] J. Carreira, E. Noland, A. Banki-Horvath, C. Hillier, and A. Zisserman, "A short note about kinetics-600," *arXiv preprint arXiv:1808.01340*, 2018.
- [427] Y. Ji, F. Xu, Y. Yang, F. Shen, H. T. Shen, and W.-S. Zheng, "A large-scale rgb-d database for arbitrary-view human action recognition," in *ACM Multimedia*.
- [428] M. Martin, A. Roitberg, M. Haurilet, M. Horne, S. Reiß, M. Voit, and R. Stiefelhagen, "Drive&act: A multi-modal dataset for fine-grained driver behavior recognition in autonomous vehicles," in *ICCV*.
- [429] H. Zhao, A. Torralba, L. Torresani, and Z. Yan, "Hacs: Human action clips and segments dataset for recognition and temporal localization," in *ICCV*.
- [430] J. Carreira, E. Noland, C. Hillier, and A. Zisserman, "A short note on the kinetics-700 human action dataset," *arXiv preprint arXiv:1907.06987*, 2019.
- [431] M. Moreaux, M. G. Ortiz, I. Ferrané, and F. Lerasle, "Benchmark for kitchen20, a daily life dataset for audio-based human action recognition," in *CBMI*.
- [432] M. Monfort, A. Andonian, B. Zhou, K. Ramakrishnan, S. A. Bargal, T. Yan, L. Brown, Q. Fan, D. Gutfreund, C. Vondrick, et al., "Moments in time dataset: one million videos for event understanding," *TPAMI*, vol. 42, no. 2.
- [433] Y. Xu, J. Yang, H. Cao, K. Mao, J. Yin, and S. See, "Arid: A new dataset for recognizing action in the dark," *arXiv preprint arXiv:2006.03876*, 2020.
- [434] W. Wang, D. Tran, and M. Feiszli, "What makes training multi-modal classification networks hard?," in *CVPR*.
- [435] T. Li, J. Liu, W. Zhang, and L. Duan, "Hard-net: hardness-aware discrimination network for 3d early activity prediction," in *ECCV*.
- [436] J. Liu, A. Shahroudy, G. Wang, L.-Y. Duan, and A. C. Kot, "Ssnet: scale selection network for online 3d action prediction," in *CVPR*.
- [437] Y. Wang, Q. Yao, J. T. Kwok, and L. M. Ni, "Generalizing from a few examples: A survey on few-shot learning," *ACM Computing Surveys (CSUR)*, vol. 53, no. 3.
- [438] H. Zhang, L. Zhang, X. Qui, H. Li, P. H. Torr, and P. Koniusz, "Few-shot action recognition with permutation-invariant attention," in *ECCV*, 2020.